

1 Detection and attribution of abrupt shift in minor periods in human- 2 impacted streamflow

3 Tian Lan ^a, Hongbo Zhang ^{b,*}, Chong-yu Xu ^c, Vijay P. Singh ^d, Kairong Lin ^e

4 ^a School of Geography and Planning, Sun Yat-sen University, Guangzhou, 510275, China;

5 ^b School of Environmental Science and Engineering, Chang'an University, Xian 710054, China;

6 ^c Department of Geosciences, University of Oslo, P.O. Box 1047, Blindern, 0316 Oslo, Norway;

7 ^d Department of Biological and Agricultural Engineering & Zachry Department of Civil Engineering, Texas A&M University, College Station 77840,
8 USA;

9 ^e School of Civil Engineering, Sun Yat-sen University, Guangzhou, 510275, China;

10

11 *Correspondence: hbzhang@chd.edu.cn

12

13

14 **Abstract:** Understanding the long-term variability of streamflow and its response to human activities in water-limited
15 areas is essential for socio-hydrologic models' development. In this study, a framework for the detection and
16 attribution of abrupt shift of minor periods in human-impacted streamflow is proposed. First, the most significant
17 abrupt shift in human-impacted streamflow is detected using the Pettitt test and verified based on different statistical
18 characteristics of streamflow series (trend, periodicity, and different quantiles) and main physical causes (main
19 reservoirs operations). According to the breakpoint, the study period was divided into approximately natural sub-
20 period and human-impacted sub-period. Interestingly, we found the "missing" of minor (2-4-year timescale) periods
21 of the runoff records after abrupt shift points in the study cases. To investigate its mechanisms, we proposed an
22 Improved Multivariate Fuzzy Mean Generating Function (IMFMGF) model to simulate the natural runoff in the
23 human-impacted period and decomposed the observed runoff into natural runoff component and human-impacted
24 changing runoff component. Then, the periodicity of these two components was compared based on Morlet wavelet
25 analysis and Ensemble Empirical Mode Decomposition (EEMD). Results showed that the minor periods' wave crests
26 and troughs of the above two components had excellent negative correspondence. The candidate mechanism is that
27 the offsetting effects (i.e., the regular anthropogenic withdrawal or intake of water.) resulted in the disappearance of
28 minor periods of the human-impacted observed, which can give more certain inputs into the prediction of non-
29 stationary streamflow series.

30 **Keywords:** Runoff; Minor periods; Abrupt change, Human activities; IMFMGF; Wei River basin

31 1 Introduction

32 Climate variability and human activities have some notable impacts on the various components of the
33 hydrological cycle (Ishak et al., 2013; Milly et al., 2002; Li et al., 2019; Chen et al., 2019; Esha & Imteaz, 2019).
34 About 31% of 145 major rivers in the world have exhibited statistically significant variations in annual streamflow
35 in recent decades (Zhai & Tao, 2017). It has been questioned that streamflow records are viewed as a stationary time
36 series. Hence, many researchers have focused on detecting the non-stationary changes in long-term hydrological time
37 series (Deng and Chen, 2017; Wang et al., 2015; Zhai and Tao, 2017). Moreover, understanding the reasons for runoff

38 variation in a changing environment is vital to coping with droughts or floods as well as to avoid unforeseen changes
39 in the future (Cassé et al., 2015). Most of the previous studies focused on the changes in mean or trend of hydrological
40 series (Feng et al., 2016; Gao et al., 2016a; Rougé et al., 2013; Zuo et al., 2012, 2016). There were various techniques
41 that have been applied to detect potential changes, such as the Mann-Kendall test, Bayesian inference, and Pettitt test
42 (Reeves et al., 2007). Wherein significant changes in mean values are defined as abrupt shifts for hydrological time
43 series (Rougé et al., 2013; Verbesselt et al., 2010). The abrupt changes can be related to some anthropogenic activities,
44 such as the construction of reservoirs and dams, streamflow regulation, the rapid increase of water consumption
45 (Cloern et al., 2016; Kam and Sheffield, 2016; Wu et al., 2017a; Zhang et al., 2015). The abrupt change point is
46 usually regarded as a breakpoint. Usually, the hydrological records before the first breakpoint are viewed to undergo
47 little influence from human interference. Conversely, the records after the breakpoint are usually disturbed by intense
48 human activities. A significant gradual trend may also occur in the non-stationary hydrological time series. The
49 relevant candidate human interferences include soil conservation, terrace construction, gradually increasing
50 population, and hydraulic engineering (Cloern et al., 2016; Kam and Sheffield, 2016; Zhang et al., 2015). Similar to
51 mean or trend, streamflow can be characterized by significantly seasonal and annual periodicities (Zhang et al., 2014).
52 Some human activities (such as hydrological regulations of reservoirs) may alter the seasonal or annual periodic
53 properties of streamflow (White et al., 2005). However, the periodic variations of streamflow due to human activities
54 received less attention, even though they play a vital role in regional water supply and hydropower generation (Koch
55 et al., 2011; Stojković et al., 2014).

56 Some studies have reported the periodicity properties or multi-timescale characteristics in hydrology,
57 meteorology, and other fields (Li et al., 2017; Wei et al., 2016; Wu et al., 2017b; Yuan et al., 2015, 2016; Zhao et al.,
58 2017). For instance, Yuan et al. (2015) found the significant 2-year to 4-year periodicities in precipitation and
59 temperature time series in the Yellow River basin. In addition, an 8-year periodicity of streamflow was significant
60 from the end of the 1960s to the beginning of the 1990s. Wei et al. (2016) applied the Morlet wavelet to analyze the
61 cycles of oscillations occurring in streamflow and suspended sediment discharge series. The cycles of oscillations
62 are mainly due to an alternate change in the wet/dry periods and the high/low sediment discharge periods in the
63 mainstream of the Yellow River. Li et al. (2017) investigated the variations of the trend, inter-annual variability, and
64 periodicity of precipitation and sunspot numbers as well as their interrelationships using Morlet wavelet analysis.
65 Results indicated that, unlike precipitation, the sunspot number reflected a clear periodic variability in the Loess
66 Plateau, China.

67 Furthermore, some gradual variations of the periodicity of time series have been of increasing concern in
68 hydrological fields. Lv et al. (2012) found that the periodicity of the runoff series presented a gradual attenuation
69 after 1965 at Huayuankou hydrological station in the Yellow River basin, China. Wu et al. (2017b) analyzed the
70 runoff records using continuous wavelet analysis. Results showed that the periodicity of the runoff was weak in the
71 1980s and strengthened after 1998. Also, this phenomenon was found in Karst hydrology by Wei et al. (2013) who
72 proposed that “the strong periodic signal attenuated and even some smaller time-scale signal disappeared in the
73 transmission process from precipitation to the spring flow through Karst aquifer”.

74 Besides the aforementioned gradual variations of the periodicity of time series, may the periodicity of
75 hydrological series occur abrupt shifts? However, there is hardly any literature discussing the abrupt shift of
76 periodicity of runoff at one or several timescales caused by anthropogenic interference. Thus, the objective of this
77 study is to propose a framework for the detection and attribution of the abrupt shift of periodicity in human-impacted
78 streamflow. What is more, although numerous current reports have concentrated on quantifying the impacts of human
79 activities and climate change on runoff variation (Bennett et al., 2016; Dey and Mishra, 2017; Deng and Chen, 2017;

80 Feng et al., 2016; Gao et al., 2015, 2016b; Jiang et al., 2015; Wang et al., 2015; Wang, 2014; Wu et al., 2017c, 2012;
81 Zhai and Tao, 2017; Zhan et al., 2014; Zuo et al., 2016), the ways human activities interfere with runoff have not
82 been explored from the perspective of periodicity. Thus, the main contribution of this study is exploring the potential
83 response mechanism for the abrupt shift of periodicity in the long-term runoff. The exploration of the response
84 mechanism is critical to the water resources planning and management but also provides essential information for
85 predicting non-stationary streamflow in complex hydro-social systems.

86 The primary novelty of this study is as shown in the following: (1) A systematic scheme for detecting and
87 verifying the abrupt shift of streamflow series is developed. (2) A framework for investigating candidate mechanism
88 of abrupt shift of minor periods in human-impacted streamflow is provided. (3) A forecast model is proposed for
89 predicting long-term natural runoff in ungauged basins.

90 **2 Study area and data**

91 The Wei River basin was selected as the study area in this paper (as shown in Figure 1). The Wei River is the
92 largest tributary of the Yellow River basin in China (Huang et al., 2017). With a total length of 818 km, its drainage
93 area is 134,800 km². The elevation of Wei River basin range spans from 320 to 3600 m above sea level and its latitude
94 range 33° 50' N-37° 18' N. The mean annual runoff is approximately 10.4 billion m³. The climatic conditions
95 are significantly different over the whole year in the Wei River basin, belonging to continental monsoon. The
96 snowmelt has a little impact on the runoff due to climate warming and winter is a very dry season (Huang et al.,
97 2017). The annual precipitation is approximately 572 mm, which is mainly concentrated in June to October. The
98 multi-year average temperature is approximately 10.6°C (Zuo et al., 2012). As a leading grain-yielding basin in
99 Northwest China, the Wei River basin is the main source of water supply, which controls the water use of 22 million
100 people. The basin, where the Guangzhong-Tianshui Economic Zone is located, plays a vital role in economic
101 development in the Northwest of China (Huang et al., 2017; Zuo et al., 2015). Over the past five decades, intensive
102 human activities, covering constructing terraces, reservoir construction, sediment-trap dams, river diversion, soil
103 conservation, and other related engineering and management practices, have caused the significant changes in the
104 long-term hydrological time series in the Wei River basin (Chen et al., 2016; Gao et al., 2013; Guo et al., 2013; Zhan
105 et al., 2014; Zuo et al., 2012; Zhao et al., 2013, 2015). Thus, the Wei River basin is appropriate for this study to
106 represent significant human-impacted basins.

107 Thirty meteorological stations and two representative hydrological gauges (including the Xianyang and
108 Zhangjiashan stations) in the Wei River basin were considered in this study (Figure 1). Precipitation and temperature
109 in each sub-area were calculated using the tessellation polygon method (Okabe et al., 2009). The Xianyang and
110 Zhangjiashan stations are located in the lower areas of the Wei River and downstream of the Jing River, respectively.
111 The datasets used in this study included mean annual precipitation, temperature, and runoff. The annual precipitation
112 and temperature data (including 1952-2009 in the Xianyang basin and 1960-2010 in Zhangjiashan basin) from 30
113 meteorological stations were collected from the National Climate Center (NCC) of the China Meteorological
114 Administration (CMA). The annual runoff records from 1934-2009 (Xianyang gauge) and 1960-2010 (Zhangjiashan
115 gauge) are provided by the Shaanxi Hydrometric and Water Resource Bureau. The sampling rate of the
116 meteorological stations and Xianyang gauge and Zhangjiashan gauge is 1-Hz and their sampling period is 1 min.

117 **3 Methodology**

118 *3.1 The framework for detection and attribution of abrupt shift of periodicity in long-term runoff series*

119 From the perspective of hydrological time series, the main statistical properties include mean, variance, trend,
120 periodicity, distribution, autocorrelation, and entropy (Hosking, 1984; Matalas, 1967; Salas, 1980; Yue et al., 2002a).
121 When human perturbation on the hydrological system (or cycle) is intensive, these properties could present varying
122 degrees of changes, and the forms of these changes mainly include abrupt change and gradual change (Machiwal et
123 al., 2017; Rougé et al., 2013). In this study, the form of abrupt change of hydrological time series was focused. In
124 this regard, it is not suggested to conclude that hydrological time series are significantly changed based on the
125 detection of sole property (such as mean or variance) in the attribution of the human disturbances. In this regard, this
126 study took the abrupt change of mean of streamflow series as the breakpoint, the significance of changes of other
127 properties (covering tendency, periodicity, and distribution) was detected before and after the abrupt change point.
128 Also, it is vital to investigate the time when intense human interference occurred to verify the above results. Most
129 importantly, it is interesting to note that the disappearance of the 2-4-year minor periods after the abrupt change point
130 and its candidate mechanisms were further explored.

131 The developed framework (Figure 2) can be summarized as follows. (1) The abrupt shift in the annual runoff
132 series was detected using the Pettitt test which is usually applied to identify the significant abrupt shift of the mean
133 value of a signal. To avoid the interference from the smooth trend, the trend-free (TF) (Yue et al., 2002a) procedure
134 is performed before the Pettitt test. Based on the detected abrupt shift point, the study period was divided into
135 approximately natural sub-period (period-1) with less anthropogenic interference and human-impacted period
136 (period-2), respectively. (2) Ensuring the effectiveness of the detected abrupt shift point under human-induced
137 hydrological change is a prerequisite for performing the following work. Hence, we applied a systematic verification
138 scheme from two different perspectives. First, the different statistical characteristics of the runoff series before and
139 after the abrupt shift were compared. Wherein, the statistical characteristics include mean, trend, periodicity, and
140 different quantiles (the minimum and maximum range values, the upper and lower quartiles, and the median). The
141 variations of the above-mentioned statistical characteristics were, respectively, detected using the Pettitt test, Trend-
142 free pre-whitening Mann-Kendall test, Morlet wavelet analysis, and boxplots techniques (see Appendix A). Second,
143 from the perspective of physical causes, we pay more attention to large-scale human activities which interfered the
144 streamflow. (3) The candidate mechanisms of abrupt change or extinction of minor periods of runoff time series are
145 investigated. First, the proposed forecast model was used to simulate the natural runoff component in the human-
146 impacted period using precipitation data and temperature data over the whole period and extracting the information
147 on runoff data before the abrupt shift. The human-impacted changing runoff component was the difference between
148 the observed runoff and the simulated natural runoff component. As a result, the observed runoff in the human-
149 impacted period was decomposed into the natural runoff component and the human-impacted changing runoff
150 component. Then, the periodic variations of these two components are compared to identify the causes of the
151 disappearance of minor periods using Morlet wavelet analysis and Ensemble Empirical Mode Decomposition (see
152 Appendix A).

153 *3.2 Improved multivariate fuzzy mean generating function model*

154 The prediction methods of natural runoff mainly include hydrological models (such as SWAT, Soil and Water
155 Assessment Tool) (Zhang et al., 2012), Restoring Water Volume (RWV) via investigating water consumption from
156 different departments, and precipitation-runoff regression model (Blöschl et al., 2013). However, there are some
157 practical limitations to these techniques. For example, the RWV approach is easily influenced by the completeness
158 and accuracy of collected data and could result in larger deviations from real natural runoff. Precipitation-Runoff
159 regression modeling is one of the most classical applications of hydrology. It simulated the river flow induced by

160 describing the relationship between the precipitation and observed runoff. The precipitation-runoff regression model
 161 is limited in areas where the precipitation-runoff relationship is weak. The hydrological models, especially spatially
 162 distributed hydrological models, have better predictive performance, but these models need to be supported by a large
 163 amount of data. Thus, this study developed a simple and practical model, termed as Improved Multivariate Fuzzy
 164 Mean Generating Function forecasting model (IMFMGF), to simulate the natural runoff on human impacts and
 165 environmental change. The basic time step of the proposed model is a year.

166 The proposed model addresses the following challenges. (1) This study detected the abrupt shift of the minor
 167 (2-4-year scale) periods in streamflow series. Actually, we found that there were no significant 2-4-year scale main
 168 periods in the precipitation series and temperature series based on the analysis of peak values of their wavelet variance
 169 at both two study sites. Hence it is vital to capture the autocorrelation and period components of streamflow series
 170 themselves. In this regard, the model was proposed and it could effectively extract the different periodic components
 171 of a signal (as well as its first-order and the second-order difference signals). (2) Second, extracted autocorrelation
 172 and periodic information of streamflow series can improve the simulation accuracy of the model. (3) Third, the
 173 advantage of the proposed forecast model is more significant when the relationship between precipitation and runoff
 174 is weak. (4) Last, the model offers better performances for forecasting extremes due to the extraction of the second-
 175 order difference signals. The peak values of the simulated streamflow are critical to periodicity analysis using the
 176 Morlet wavelet (Bayazit et al., 2001). Its algorithm is composed of the following steps (see Figure 3).

177 *Step 1. Design exponentially increasing Membership Function:*

$$\mu_A = e^{-\beta(n-t)} (t = 1, \dots, n) \quad (1)$$

178 where μ_A is the membership degree with time t ; n is the length of the signal x ; β is the fuzzy membership parameter
 179 which is usually set to 0.01.

180 *Step 2. Calculate Fuzzy Mean Generating Function (FMGF):*

$$\bar{x}_l(i) = \frac{\sum_{j=0}^{n_l-1} \mu_A(X) \cdot x(X)}{n_l} (i = 1, \dots, l; 1 \leq l \leq m) (X = \text{REM}(n, l) + i + jl) \quad (2)$$

$$n_l = \text{INT}\left(\frac{n}{l}\right); m = \text{INT}\left(\frac{n}{2}\right)$$

181 where l is the time-interval sequence; $\text{REM}(n, l)$ returns the remainder after the division of n by l ; $\text{INT}(n/l)$
 182 returns the signed integer after the division of n by l .

183 *Step 3. Calculate Extended Fuzzy Mean Generating Function (EFMGF):*

$$f_l(t) = \bar{x}_l(i), \text{mod}(t, l) \equiv \text{mod}(i, l) (t = 1, 2, \dots, n) \quad (3)$$

184 where $\text{mod}(t, l)$ returns the modulus after the division of t by l .

185 *Step 4. Calculate the EFMGFs of the first-order difference signal and second-order difference signal:*

$$\Delta x(t) = x(t+1) - x(t) (t = 1, \dots, n-1) \quad (4)$$

$$\Delta^2 x(t) = \Delta x(t+1) - \Delta x(t) (t = 1, \dots, n-2) \quad (5)$$

186 The EFMGFs of the original signal, the first-order difference signal, and the second-order difference signal are
 187 $f_l^{(0)}(t)$, $f_l^{(1)}(t)$, $f_l^{(2)}(t)$, respectively. All the EFMGFs are regarded as predictive factors.

188 *Step 5. Optimize the predictive factors by applying the screening criteria based on the variance analysis.*

$$Z = \frac{S(l)}{l} \quad (6)$$

$$S(l) = \sum_{i=0}^l n_i (\bar{x}_l(i) - \bar{x})^2 \quad (2 \leq l \leq m) \quad (7)$$

189 All the predictive factors are sorted according to their corresponding Z values. The first P predictive factors are
 190 selected as the final predictive factors. In general, the range of the P -value is 3 to 5.

191 *Step 6:* Add K external predictive factors, such as precipitation and temperature. Multiple regression model is
 192 estimated as follows:

$$\hat{x}(t) = a_0 + \sum_{i=1}^{P+K} a_i f_i(t) \quad (8)$$

193 where $\hat{x}(t)$ is the simulations; a_0 and a_i are the regression parameters; $f_i(t)$ is the i^{th} predictive factors.

194 The classical mean generating function (MGF) was proposed by Cao and Wei (1991). The fuzzy mean generating
 195 function (FMGF) was subsequently developed by means of a Membership Function, which can represent the fuzzy
 196 behavior of this algorithm. The exponentially increasing Membership Function is designed to maximize the
 197 effectiveness of the latest data of the signal because the latest data play a more critical role in long-term prediction.
 198 The FMGF can extract the different periodic components of the signal. However, the latest data of the signal are
 199 usually not effectively used in the FMGF. Hence, we construct the FMGF based on the reverse-order signal (Zuo and
 200 Gao, 2004). The same operations are performed in the first-order and the second-order difference signals to fit the
 201 high-frequency components of the signal. The verification of the proposed model is elaborated as follows.

202 **4 Results and discussion**

203 *4.1 Detecting and verifying the abrupt change of long-term runoff*

204 The results of the Pettitt test (see Figure 4) are that the most significant abrupt shift point of mean values of the
 205 annual runoff time series is at Xianyang gauge in 1972 (Figure 5(a)) and at Zhangjiashan gauge in 1998 (Figure 5(c)).
 206 The streamflow series in the period-1 (before the abrupt change point) and period-2 (after the abrupt change point)
 207 are redetected using the Pettitt test to reconfirm whether the streamflow in the natural period (period-1) existed the
 208 intense human interference. The results showed that there are no significant abrupt change points in the streamflow
 209 series in Period-1 at both two study sites. In period-2, there is no significant abrupt change point at Zhangjiashan
 210 gauge, and a significant abrupt shift point in 1995 exists in the streamflow series at Xianyang gauge. The results
 211 demonstrated that in 1972, it was not only the most significant abrupt change point of the measured runoff at
 212 Xianyang gauge but also the first abrupt shift point. This situation at Zhangjiashan gauge was the same as that at
 213 Xianyang gauge. The detected abrupt shift points are verified from the following perspectives.

214 (1) The statistical characteristics from boxplot (including maximum value, first quartile (25%), mean, third
 215 quartile (75%), and minimum value of data) between the observed runoff series in period-1 and period-2 were
 216 compared, as shown in Figure 5(b). The figures show that these characteristic values of annual runoff in period-2
 217 decreased at Zhangjiashan gauge. Notably, the 25-75% intervals of data could effectively represent the variance of
 218 series, which were also significantly narrowed. Furthermore, a more rigorous statistical test, i.e., KS test for the
 219 difference between the distribution of the series in period 1 and period 2. The results that the null hypothesis at the

220 1% significance level is not rejected, which indicated that the distributions of these two series (streamflow series in
221 period 1 and period 2) are significantly different. In addition, the length of data after the abrupt shift point at
222 Zhangjiashan gauge is not applicable to the boxplot.

223 (2) The significance of the trend of runoff series in period-1 and the entire period was detected and compared
224 using TFPW-MK (i.e., Trend-free pre-whitening Mann-Kendall test) at the different significant level (0.001, 0.005,
225 0.01, 0.05, 0.1, 0.5). The results (see Table 1) showed that the observed runoff series in period-1 at both two study
226 sites have no significant trend. For the entire period, the results manifested that both the runoff series in the whole
227 period at both two study sites significantly decreased at a different significance level. It indicated that the sharp
228 reduction after the abrupt change point leads to the results of the MK test for the whole series, i.e., a significant trend.
229 This further validated the results of Pettitt's test. It is worth noting that the significant trend tested by MK is likely
230 not smooth because non-parametric MK test converts original time series to ranks, which can only be used to illustrate
231 the monotonicity of monotonic series (Hamed, 2008; Hamed and Ramachandra Rao, 1998; Yue et al., 2002a). Also,
232 the results of the TFPW-MK test in period-1 and the entire period were consistent with the results of other relevant
233 literature (Guo et al., 2013; Zhan et al., 2014; Zuo et al., 2012).

234 (3) For periodicity properties, we apply Morlet wavelet analysis to reveal the changes in frequency components
235 of observed runoff series in different time domains. The modulus and the real part of the wavelet transform
236 coefficients are two important factors. The modulus represents the energy density of the signal because the energy is
237 in direct ratio to the modulus. The real part of wavelet transform coefficients denotes the distribution of the signal
238 phase in the time domain. In the hydrological system, the Morlet wavelet transform coefficients can characterize the
239 multi-scale evolution and the transient properties of hydrological processes. The positive value of the real part
240 corresponds to the wet period, the negative value corresponds to the drought period, and the zero corresponds to the
241 transitional area (Hao et al., 2012; Zhang et al., 2007). In this regard, the real part of the wavelet coefficient contour
242 maps of runoff is used to analyze the variations of periodicity properties of runoff time series in this study. The real
243 parts of the wavelet coefficient contour maps of the observed runoff and their schematics in minor periods at the
244 Xianyang gauge and Zhangjiashan gauge are shown in Figure 6. It can be seen that ① the 25-year main period of
245 runoff was shortened to the 20-year period over time. This phenomenon indicated that the low-frequency runoff
246 exhibited a gradually decreasing trend, which was consistent with the results of the TFPW-MK test at both gauges;
247 ② at Xianyang gauge, the 9-year main period of the observed runoff first reduced and then expanded, next to more
248 irregular after 2000. However, the 9-year main period of the observed runoff was more steady at Zhangjiashan gauge;
249 ③ Most notably, the significant 2-4 year minor periods of the runoff series disappeared after the abrupt shift point
250 at both two gauges, which is further discussed below. The wavelet variance for the observed streamflow is usually
251 used to identify the main periodic components (Jenouvrier et al., 2005; Li et al., 2013; Nakken, 1999). So, we utilize
252 the wavelet variance for after and before abrupt change point of observed streamflow to verify the disappearance of
253 the minor periods of human-impacted observations. As shown in Figure 7, the results showed that the minor periods
254 (2-4-year timescale) disappeared after the significant abrupt change points at both two sites.

255 (4) Indeed, any method of detecting hydrological change cannot be viewed as convincing evidence (Buishand,
256 1984). Hence the main human interference (such as the reservoirs regulations) were further investigated. In the Wei
257 River basin, the reservoirs are the largest human disturbance (Zhan et al., 2014). It is important to emphasize the
258 operation mode of the reservoir system. The large-scale surface water withdrawals from the reservoirs are used to
259 irrigation fields, industrial, and domestic water consumption (Zhan et al., 2014). Hence, the construction of reservoirs
260 not only redistributes the seasonal water discharge within any given year but also significantly adjusts inter-annual
261 distribution. The inter-annual distribution is identified by two important indices including the completion time and

262 storage capacities of the main reservoirs, which are visualized in Figure 8. In the upstream of the Xianyang gauge,
263 the main reservoirs with relatively large reservoir capacity include Jinping reservoir, Xiazhai reservoir,
264 Zhangjiazitou reservoir, Duanjiaxia reservoir, Fengjiashan reservoir, Shituhe reservoir, Xinyigou reservoir,
265 Yangmaowan reservoir, Dabeigou reservoir, Laoyaju reservoir, and Shibianyu reservoir. According to the colors of
266 the bubble chart, most of them were built simultaneously in the early 1970s. In the Jing River basin, the largest
267 reservoir, Xijiao reservoir, was constructed in 1997. It directly controls the streamflow volume in the downstream of
268 the Zhangjiashan gauge. Besides, some water withdrawal from the river channel for regional agriculture, industry,
269 and human life caused the approximate doubling of a decrease in the early 1970s in the mainstream of the Wei River
270 basin. As a result, the interference time of the main human activities in the study areas is close to the abrupt shift
271 point of runoff, which further verified the above results.

272 *4.2 Natural runoff simulating*

273 To explore the candidate mechanisms of abrupt change or the disappearance of minor periods of the runoff time
274 series in the study areas, we decomposed the observed runoff into the natural runoff component and human-impacted
275 runoff component which mainly reflected water intake or water consumption by human activities. Hence, it is vital
276 for simulating natural runoff.

277 *4.2.1 Verification of the IMFMGF model in the natural period*

278 The annual runoff series at Xianyang gauge was taken as an example to verify the IMFMGF (i.e., Improved
279 Multivariate Fuzzy Mean Generating Function) model. The hydrological data (including annual precipitation,
280 temperature, and runoff data) in 1953-1964 and in 1965-1971 were used for the calibration and verification of the
281 model, respectively. In the proposed model, the optimized predictive factors and their corresponding regression
282 parameters and Z values are listed in Table 2. The simulated natural runoff is shown in Figure 9. The model
283 performance in the calibration and verification periods is evaluated using the Nash Sutcliffe efficiency coefficient
284 (NSE) (Nash and Sutcliffe, 1970), and their NSE values are 0.971 and 0.892, respectively. The result shows that the
285 model performance for simulating natural runoff is good. Furthermore, the model performance in the peaks is
286 evaluated using the Mean Relative Errors (MRE) metric (Islamoglu, 2003). Wherein the peaks are extracted using
287 the built-in findpeaks MATLAB function (Ferraris et al., 2014), which are marked in red in Figure 9. The MRE values
288 of the extreme points in the validation period is 0.153, which indicates that the model has an advantage in simulating
289 extremum.

290 *4.2.2 Verification of the IMFMGF model in the human-impacted period*

291 Considering there is no measured natural runoff in the human-impacted period that can be referred, the simulated
292 natural runoff is verified in three different ways: (1) the different statistical characteristics of the observed natural
293 runoff and the simulated natural runoff are compared, which are represented using the boxplots in Figure 10. The
294 observed natural runoff denotes the observed runoff before the abrupt change point (1933-1971). The simulated
295 natural runoff denotes the simulated runoff after the abrupt change point (1972-2009). As shown in Figure 10, these
296 statistical characteristics and the intervals of these two series are with no significant difference. (2) The precipitation-
297 natural runoff relationship can comprehend the tremendous spatial and temporal watershed characteristics, snowpack
298 or precipitation patterns, as well as other complex hydrological phenomena (Tokar and Johnson, 1999). Hence, it is
299 also used to verify the simulated natural runoff by determining whether the precipitation-runoff relationship was
300 stable before and after the abrupt change point. See Figure 11, the regression lines of the precipitation-natural runoff

301 scatter plot before and after the abrupt change was close. Their correlation coefficients (R^2) are 0.846 and 0.901,
302 respectively, which are also close. (3) The simulation accuracy of hydrological time series is sensitive to its high-
303 frequency components (i.e., minor periods) (Karthikeyan and Nagesh Kumar, 2013). Hence, we analyzed the contour
304 maps of the real part wavelet coefficients of the simulated natural runoff components to further verify the model
305 performance. In Figure 12, the 2-4-year main periods of the simulated natural runoff were restored and their regular
306 distributions were consistent with the distributions of the observed natural runoff in the natural period. Consequently,
307 with the limitation of the absence of the observed natural runoff in the human-impacted period, the three different
308 verification processes suggest that the proposed model for simulating natural runoff is robust.

309 The predicted results and the observed values at both two study cases are drawn in Figure 13. The Nash-Sutcliffe
310 efficiency coefficient values for the simulated natural streamflow in the natural period at Xianyang gauge and
311 Zhangjiashan gauge are 0.958 and 0.889, respectively. Moreover, in the natural period (period-1), the NSE value for
312 simulated and observed runoff is 0.971 in the calibration period and 0.892 in the verification period. In the human-
313 impacted period (period-2), the NSE for simulated natural runoff and observed runoff is 0.958 in the period-1 and
314 0.413 in the period-2. As a result, the difference between the calibration and simulation in period-1 and period-2 is
315 large. It indicates that the effect of model errors on simulated runoff is insignificant compared to the interference of
316 human activities on observed runoff.

317 *4.3 Effect of climatic conditions on the streamflow*

318 (1) The precipitation and temperature datasets at two study areas are visualized, as shown in Figure 14. The
319 stationarity of precipitation and temperature is assessed using TFPW-MK. The results (see Table 3) show that the
320 precipitation time series in both study areas have no significant trend, but the temperature time series have a
321 significant upward gradient. It is worth emphasizing that the changes in the temperature time series are gradual rather
322 than abrupt. (2) On the one hand, the main climate factor which controls the runoff generation is precipitation. The
323 MK test results showed that the precipitation time series is stationary. The temperature time series with a gradual
324 upward trend control the regional evapotranspiration. The increase in evaporation is insignificant compared to the
325 variation of runoff caused by human activities in the study areas (Huang et al., 2016; Wu et al., 2017c; Zhan et al.,
326 2014; Zou et al., 2018). (3) On the other hand, the objective of this study is actually the detection and attribution of
327 abrupt shifts in minor periods in human-impacted streamflow. Hence, the form of the abrupt change of the streamflow
328 time series was focused rather than a gradual shift. The large-scale human activities, which may cause the abrupt
329 changes of runoff, were investigated to explore the mechanism of the abrupt shift in minor periods. The reservoir
330 system is the largest human disturbance in the Wei River basin (Zhan et al., 2014). It is important to emphasize the
331 operation mode of the reservoir system. The large-scale surface water withdrawals from the reservoirs are used to
332 irrigation fields, industrial, and domestic water consumption (Zhan et al., 2014). The inter-annual distribution is
333 identified by two important indices including the completion time and storage capacities of the main reservoirs. The
334 volume of stored water along the time is difficult to be collected in this study, which is one of the limitations of this
335 study and the future work needs to be considered. (4) Furthermore, the proposed forecasting model for the natural
336 runoff after the abrupt change point used the precipitation and temperature as two of prediction factors. That is, the
337 forecasted natural runoff involved the variation of climate conditions only. The negative values of measured minus
338 simulated runoff which is human-impacted runoff component reveals the human-impacted changing runoff
339 corresponds to human-induced water withdrawal. (5) Moreover, it was found that there were no significant 2-4-year
340 scale main periods in the precipitation series and temperature series based on the analysis of peak values of their
341 wavelet variance. Excluding the effects of the variations in climatic conditions on the abrupt shift of the minor periods

342 of the runoff, we focus on exploring the potential mechanism considering the effects of human activities.

343 *4.4 Mechanism of abrupt shift in minor periods in human-impacted streamflow*

344 Here, the periodicity properties of the natural runoff component and the human-impacted runoff component
345 were compared via Morlet wavelet analysis and EEMD (i.e., Ensemble empirical mode decomposition) techniques.
346 The contour maps of the real part wavelet coefficients of the two components at Xianyang and Zhangjiashan gauges
347 are shown in Figure 12. According to the schematics in their minor periods, it is interesting to note that the wave
348 crests and troughs of the two components in 2-4-year minor periods have good negative correspondence. Specifically,
349 when the minor periods of natural component series are in the troughs, the minor periods of human-impacted runoff
350 components are at the peaks, and vice versa. The referred potential mechanism is that the larger the amount of natural
351 water was, correspondingly, the more the anthropogenic water withdrawal was. Indeed, in the wavelet analysis
352 algorithm, selecting a different mother wavelet would affect the outcome (Zhang et al., 2016). Hence, the stability of
353 the results of the wavelet analysis needs to be further verified. In this regard, we further used EEMD (i.e., Ensemble
354 empirical mode decomposition) method to filter out the long-term background change of the runoff time series and
355 extract the high-frequency components (Intrinsic Mode Functions, IMFs) from the natural runoff and human-
356 impacted runoff. The results (see Figure 15) indicated that the relationships between crests and troughs of the IMFs
357 from the natural runoff and the human-impacted runoff were consistent with the above results from Morlet wavelet
358 analysis.

359 Our preliminary analysis indicates that the response of the abrupt shift of minor periods of long-term runoff to
360 human activities in the human-impacted period was an objective existence in the Wei River basin. The human-
361 impacted runoff component was at the same frequency with the natural runoff in opposite directions. One candidate
362 mechanism for the abrupt shift of minor periods in the Wei River basin, we suggest, is the regular anthropogenic
363 disturbance in the annual runoff, i.e., the regular anthropogenic withdrawal or intake of water (more water was
364 withdrawn in wet years, and the less water was withdrawn in dry years). The offsetting effects in the 2-4-year minor
365 periods resulted in the disappearance of minor periods of observed runoff in the human-impacted period. The effective
366 benefits coming from the discussion of the potential mechanism of abrupt shift in minor periods in human-impacted
367 streamflow are that the abrupt changes of the components in the frequency domain can provide the variable references
368 for the inputs of simulating models. The identified variational periodicity properties as the inputs can significantly
369 increase the prediction accuracy of hydrological models in non-stationary hydrological regime (Yaseen et al., 2016).
370 Also, the attribution can provide vital information for building the coupled human-water systems in socio-hydrologic
371 models (Elshafei et al., 2015; Troy et al., 2015).

372 **5 Conclusions**

373 A framework for the detection and attribution of abrupt shift of minor periods in human-impacted streamflow
374 was proposed and applied at two hydrological gauges in the Wei River basin, China. The framework provides vital
375 information in socio-hydrologic models and gives more certain inputs into the prediction of non-stationary
376 hydrological time series in the changing natural and social environment. The main contributions can be drawn:

- 377 1. The most significant abrupt shift in human-impact streamflow in the study areas was detected by the Pettitt test.
378 It was effectively verified by a systematic verification scheme including trend, periodicity, different quantiles,
379 and main physical causes.
- 380 2. It is found that the significant 2-4-year minor periods of the runoff series disappeared after the abrupt shift point
381 in the study cases. The candidate mechanism was investigated that the offsetting effects (i.e., the regular

382 anthropogenic withdrawal or intake of water) resulted in the disappearance of the minor periods of observed
383 runoff in the human-impacted period. The exploration of the mechanism of this phenomenon is implemental to
384 develop socio-hydrologic models and simulate the non-stationary hydrological time series.

385 3. The proposed model for simulating the long-term natural runoff (i.e., Improved Multivariate Fuzzy Mean
386 Generating Function) addressed the three challenges including the extraction of autocorrelation and periodic
387 information of streamflow series, application for the area where the relationship between precipitation and runoff
388 is weak and data are poor, and robust extreme point predictions. Additionally, the uncertainty in the proposed
389 model needs to be further considered and supplemented.

390 **Acknowledgments**

391 The work described in this paper was supported financially by the National Natural Science Foundation of China
392 (51379014), the Major Program of the National Natural Science Foundation of China (41790441), the Technology
393 Foundation for Selected Overseas Chinese Scholars, Department of Personnel in Shaanxi Province of China
394 (2017035), and the Research Council of Norway (FRINATEK Project 274310), which are greatly appreciated. Our
395 deepest gratitude goes to Prof. Xu for his great work and professional guidance that have helped improve this revision
396 substantially, especially in the *Results*, *Discussion*, and *Conclusions* sections. The authors would like to thank the
397 comments of the editors and four anonymous reviewers which significantly improved the quality of this manuscript.

398 **Appendix A**

399 *Pettitt test*

400 The Pettitt test detects the change points of the mean values of signals against the null hypothesis on the initial
401 distribution. It is based on the Mann and Whitney statistical function ($U_{t,T}$) for comparing two independent samples
402 (x_1, \dots, x_t) and (x_{t+1}, \dots, x_T) and gives the date of change point (Fraedrich et al., 2001; Kam and Sheffield, 2016;
403 Pettitt, 1979; Serinaldi et al., 2018). $U_{t,T}$ is computed by:

$$U_{t,T} = U_{t-1,T} + V_{t,T} \quad (t = 2, \dots, T) \quad (9)$$

$$V_{t,T} = \sum_{j=1}^T \text{sgn}(x_t - x_j) \quad (10)$$

$$\text{sgn}(x) = \begin{cases} -1, & x < 0 \\ 0, & x = 0 \\ +1, & x > 0 \end{cases} \quad (11)$$

404 The most significant change point is evaluated by:

$$p(t) = \max |U_{t,T}| \quad (12)$$

405 The significant probability associated with potential change point is approximated by:

$$q(t) \approx 2 \cdot \exp\left(\frac{-6U_{t,T}^2}{T^3 + T^2}\right) \quad (13)$$

406 *Trend-free pre-whitening Mann-Kendall test*

407 The non-parametric Mann-Kendall (MK) statistical test recommended by WMO (World Meteorological
 408 Organization) has been widely used to determine the significance of trend in hydrological time series (Douglas et al.,
 409 2000; Hamed and Rao, 1998; Kendall, 1975; Mann, 1945; Yue et al., 2002b; Yue and Wang, 2004). The Mann-
 410 Kendall test statistic can be stated as follows:

$$S = \sum_{i=1}^{n-1} \sum_{j=i+1}^n \text{sgn}(x_j - x_i), \text{ and } \text{sng}(\theta) = \begin{cases} +1 & \theta > 0 \\ 0 & \theta = 0 \\ -1 & \theta < 0 \end{cases} \begin{cases} +1, \theta > 0 \\ 0, \theta = 0 \\ -1, \theta < 0 \end{cases} \quad (14)$$

411 where x_j and x_k are the sequential values at times j and k , respectively, and n is the length of the data set.

412 With an asymptotically normal distribution, the mean and variance are given by

$$E(S) = 0, \text{ and } \text{Var}(S) = [n(n-1)(2n+5)]/18 \quad (15)$$

413 The standard normal Z -test statistic is computed by

$$Z = \begin{cases} \frac{S-1}{\sqrt{\text{Var}(S)}} & S > 0 \\ 0 & S = 0 \\ \frac{S+1}{\sqrt{\text{Var}(S)}} & S < 0 \end{cases} \quad (16)$$

414 When $|Z| \leq Z_{1-\alpha/2}$ at the α level of significance, the null hypothesis is accepted. $Z_{1-\alpha/2}$ is the critical value
 415 of Z from the standard normal table, the value of $Z_{1-\alpha/2}$ is 1.96 for 5% significant level. Positive Z value means
 416 an increasing trend, while negative Z value means a decreasing trend (Douglas et al., 2000).

417 The autocorrelation of the runoff series has a negative effect on the results of the MK test. Thus, the hydrological
 418 time series showing significant serial correlation effects were subjected to trend-free pre-whitening (TFPW)
 419 procedures before applying the MK test (Aziz and Burn, 2006; Serinaldi and Kilsby, 2016; Wu et al., 2016; Yue et
 420 al., 2003, 2002b). The TFPW procedure first estimated the value of trend slope to remove the trend component in the
 421 series, and then estimated ρ_1 (the lag-1 data autocorrelation coefficient) so as to reduce or eliminate the serial
 422 correlation by removing the AR(1) component from the detrended series, and finally reinstalled the trend component
 423 before applying the MK test.

424 *Morlet wavelet analysis*

425 Wavelet analysis is a time-frequency decomposition technique. Comparing simple frequency analysis (e.g.
 426 Fourier analysis), wavelets transform can extract the dominant modes of variability from time series and reveal the
 427 localized time and frequency information at different timescales. The Fourier transform assumes that the signal is
 428 stationary and that the signals in the sample continue into infinity. However, it performs poorly when this is not the
 429 case. Wavelets perform better for non-stationary and non-smooth time series (Labat, 2005; Labat et al., 2000; Morlet
 430 et al., 1982; Partovian et al., 2016; Torrence and Webster, 1998; Werner, 2008). Hence, wavelet analysis is used to
 431 detect the variations of the frequency distribution of non-stationary series. The continuous wavelet transform
 432 $C_X(a, \tau)$ of $x(t)$ is defined as follows:

$$C_X(a, \tau) = \int_{-\infty}^{\infty} x(t) \Psi_{a,\tau}(t) dt = \langle x(t) \Psi_{a,\tau}(t) \rangle \quad (17)$$

$$\Psi_{a,\tau}(t) = |a|^{-0.5} \Psi\left(\frac{t-\tau}{a}\right), a, \tau \in R, a \neq 0 \quad (18)$$

433 Where a and τ are scale and time variables, respectively; $\Psi_{a,\tau}(t)$ denotes the wavelet family generated by
 434 continuous translation and dilation of the mother wavelet $\Psi(t)$.

435 Because Morlet wavelet provides a good balance between time and frequency localization (Hao et al., 2012),
 436 Here, Morlet wavelet is applied as mother wavelet and its definition as follows:

$$\Psi(t) = e^{iw_0 t} e^{-t^2/2} \quad (19)$$

437 Where w_0 is a constant. For $w_0 \geq 5$, the Morlet wavelet can approach the admissible condition.

438 The wavelet spectrum $W_X(a, \tau)$ of $x(t)$ is defined as the modulus of its wavelet coefficients:

$$W_X(a, \tau) = C_X(a, \tau) C_X^*(a, \tau) = |C_X(a, \tau)|^2 \quad (20)$$

439 Where $C_X(a, \tau)$ and $C_X^*(a, \tau)$ are the conjugate of the wavelet coefficient of X (Labat, 2010).

440 *Ensemble empirical mode decomposition*

441 The ensemble empirical mode decomposition (EEMD) is the extension of EMD (Empirical Mode
 442 Decomposition) (Huang et al., 1998). EEMD combines a noise-assisted adaptive data analysis algorithm. In the
 443 process of implementing EEMD, white noise is added to the original noise to eliminate the mode mixing problem
 444 (Antico, Schlotthauer, & Torres, 2014; Torres, Colominas, Schlotthauer, & Flandrin, 2011; Z. Wu & Huang, 2009).
 445 The trial is that the modified signal inputs EMD, which is repeated m times to obtain the final mode. The theoretical
 446 frame of the EEMD method is:

$$x_m(t) = x(t) + w_m(t), m = 1, 2, \dots, N \quad (21)$$

$$x_m(t) = \sum_{i=1}^l + r_{m,i}(t), m = 1, 2, \dots, N \quad (22)$$

$$x(t) = \frac{1}{N} \sum_{i=1}^l \sum_{m=1}^N c_{m,i}(t) + \frac{1}{N} \sum_{m=1}^N r_{m,i}(t) \quad (23)$$

447 where $x(t)$ is the original signal, $w_m(t)$ is the m th adding white Gaussian noise, $c_{m,i}(t)$ is the i th IMF of the m th
 448 trial, l is the number of IMFs based on the EMD method, and N is the ensemble number of the EEMD method.

449 **Appendix B**

450 *Dataset size for the statistical tests*

451 The feasibility of dataset size for the statistical tests is discussed. (1) The length of datasets for precipitation,
 452 temperature, and runoff in the study areas is emphasized in the revision, as shown in Table 4. (2) The Pettitt test based
 453 on the Mann and Whitney statistical function requires large enough sample sizes (> 30) (Pettitt, 1979). In this study,
 454 the length of annual streamflow time series is 76 years in Xianyang gauge and 79 years in Zhangjiashan gauge which
 455 is feasible for Pettitt test. (3) The minimum number of samples that can be analyzed using the Mann-Kendall test is

456 17 (Mann, 1945; Pettitt, 1979; Yue and Wang, 2004). In this study, the length of whole streamflow time series is 76
457 years in Xianyang gauge and 79 years in Zhangjiashan gauge. The length of streamflow time series before the abrupt
458 change point at both gauges is 38 years. Hence, it is feasible to the application of Mann-Kendall test. (4) The
459 applications of Morlet wavelet analysis with continuous wavelet transform and Ensemble Empirical Mode
460 Decomposition (EEMD) are not limited by the sample size (Flandrin et al., 2004; Grossmann et al., 1990; Lin and
461 Qu, 2000; Wu and Huang, 2009). Moreover, the significant 2-4-year minor periods of the runoff series were focused
462 in this study. Hence, the length of the whole streamflow time series and the streamflow after the abrupt change point
463 at both gauges is workable for Morlet wavelet analysis and EEMD. (5) Moreover, the boundary effects in Morlet
464 wavelet analysis and EEMD are eliminated to overcome the limitation of definite sample size. Padding, one of the
465 simplest and effective methods for ameliorating the edge effect of continuous wavelet transform (Boltežar and Slavič,
466 2004), was applied for Morlet wavelet analysis in the revision. The wave extension method proposed by (Coughlin
467 and Tung, 2004) was utilized to handle the edge effects of EEMD. (6) The proposed statistical hydrological model
468 based on fuzzy mean generating function is designed by extracting the effective periodic components from
469 streamflow time series. Its basic structure is multiple regression model which requires a minimum sample size of 30
470 (Kutner et al., 2005). Accordingly, the 70 points are sufficient to assess the proposed model.

471 **References**

- 472 Aziz, O.I.A., Burn, D.H., 2006. Trends and variability in the hydrological regime of the Mackenzie River Basin. *J. Hydrol.*, 319(1-4):
473 282-294. <https://doi.org/10.1016/j.jhydrol.2005.06.039>
- 474 Bayazit, M., ÖNÖZ, B., Aksoy, H., 2001. Nonparametric streamflow simulation by wavelet or Fourier analysis. *Hydrolog. Sci. J.*, 46(4):
475 623-634. <https://doi.org/10.1080/02626660109492855>
- 476 Bennett, J.C., Wang, Q.J., Li, M., Robertson, D.E., Schepen, A., 2016. Reliable long-range ensemble streamflow forecasts: Combining
477 calibrated climate forecasts with a conceptual runoff model and a staged error model. *Water Resour. Res.*, 52(10): 8238-8259.
478 <https://doi.org/10.1002/2016wr019193>
- 479 Blöschl, G., Sivapalan, M., Wagener, T., Viglione, A., Savenije, H., 2013. *Runoff prediction in ungauged basins*. Cambridge University
480 Press. <https://doi.org/10.1017/CBO9781139235761>
- 481 Boltežar, M., Slavič, J., 2004. Enhancements to the continuous wavelet transform for damping identifications on short signals. *Mech.*
482 *Syst. Signal Pr.*, 18(5): 1065-1076. DOI:<https://doi.org/10.1016/j.ymsp.2004.01.004>
- 483 Buishand, T.A., 1984. Tests for detecting a shift in the mean of hydrological time series. *J. Hydrol.*, 73(1): 51-69.
484 [https://doi.org/10.1016/0022-1694\(84\)90032-5](https://doi.org/10.1016/0022-1694(84)90032-5)
- 485 Cao, H.X., Wei, F.Y., 1991. A method of time series analysis based on a mean generating function. *J. Numer. Method Comput. Appl.*,
486 12(2): 82-89. (in Chinese)
- 487 Cassé, C., Gosset, M., Alkaly Tanimoun, B., 2015. Analysis of hydrological changes and flood increase in Niamey based on the
488 PERSIANN-CDR satellite rainfall estimate and hydrological simulations over the 1983–2013 period. *PIAHS*, 370: 117-123.
489 <https://doi.org/10.5194/piahs-370-117-2015>
- 490 Chen, L., Chang, J., Wang, Y., Zhu, Y., 2019. Assessing runoff sensitivities to precipitation and temperature changes under global climate-
491 change scenarios. *Hydrol. Res.*, 50(1): 24-42. <https://doi.org/10.2166/nh.2018.192>
- 492 Chen, X., Su, Y., Liao, J., Shang, J., Dong, T., Wang, C., Liu, W., Zhou, G., Liu, L., 2016. Detecting significant decreasing trends of land
493 surface soil moisture in eastern China during the past three decades (1979–2010). *J. Geophys. Res. Atmos.*, 121(10): 5177-5192.
494 <https://doi.org/10.1002/2015jd024676>
- 495 Cloern, J.E., Abreu, P.C., Carstensen, J., Chauvaud, L., Elmgren, R., Grall, J., Greening, H., Johansson, J.O.R., Kahru, M., Sherwood,
496 E.T., Xu, J., Yin, K., 2016. Human activities and climate variability drive fast - paced change across the world's estuarine - coastal

497 ecosystems. *Glob. Chang. Biol.*, 22(2): 513-529. <https://doi.org/10.1111/gcb.13059>

498 Coughlin, K.T., Tung, K.K., 2004. 11-Year solar cycle in the stratosphere extracted by the empirical mode decomposition method. *Adv.*
499 *Space Res.*, 34(2): 323-329. DOI:<https://doi.org/10.1016/j.asr.2003.02.045>

500 Deng, H.J., Chen, Y.N., 2017. Influences of recent climate change and human activities on water storage variations in Central Asia. *J.*
501 *Hydrol.*, 544: 46-57. <https://doi.org/10.1016/j.jhydrol.2016.11.006>

502 Dey, P., Mishra, A., 2017. Separating the impacts of climate change and human activities on streamflow: A review of methodologies and
503 critical assumptions. *J. Hydrol.*, 548: 278-290. <https://doi.org/10.1016/j.jhydrol.2017.03.014>

504 Douglas, E.M., Vogel, R.M., Kroll, C.N., 2000. Trends in floods and low flows in the United States: impact of spatial correlation. *J.*
505 *Hydrol.*, 240(1): 90-105. [https://doi.org/10.1016/S0022-1694\(00\)00336-X](https://doi.org/10.1016/S0022-1694(00)00336-X)

506 Elshafei, Y., Coletti, J.Z., Sivapalan, M., Hipsey, M.R., 2015. A model of the socio-hydrologic dynamics in a semiarid catchment:
507 Isolating feedbacks in the coupled human-hydrology system. *Water Resour. Res.*, 51(8): 6442-6471.
508 <https://doi.org/10.1002/2015WR017048>

509 Esha, R.I., Imteaz, M.A., 2019. Assessing the predictability of MLR models for long-term streamflow using lagged climate indices as
510 predictors: a case study of NSW (Australia). *Hydrol. Res.*, 50(1): 262-281. <https://doi.org/10.2166/nh.2018.171>

511 Fasano, G., Franceschini, A., 1987. A multidimensional version of the Kolmogorov–Smirnov test. *Mon. Not. R. Astron. Soc.*, 225(1):
512 155-170. <https://doi.org/10.1093/mnras/225.1.155>

513 Feng, X.M., Cheng, W., Fu, B.J., Lu, Y.H., 2016. The role of climatic and anthropogenic stresses on long-term runoff reduction from the
514 Loess Plateau, China. *Sci. Total Environ.*, 571: 688-98. <https://doi.org/10.1016/j.scitotenv.2016.07.038>

515 Ferraris, C., Nerino, R., Chimienti, A., Pettiti, G., Pianu, D., Albani, G., Azzaro, C., Contin, L., Cimolin, V., Mauro, A., 2014. Remote
516 monitoring and rehabilitation for patients with neurological diseases, Proceedings of the 9th International Conference on Body Area
517 Networks. ICST (Institute for Computer Sciences, Social-Informatics and Telecommunications Engineering), London, United
518 Kingdom, pp. 76-82. <https://doi.org/10.4108/icst.bodynets.2014.257005>

519 Flandrin, P., Rilling, G., Goncalves, P., 2004. Empirical mode decomposition as a filter bank. *IEEE Signal Proc. Let.*, 11(2): 112-114.
520 DOI:10.1109/LSP.2003.821662

521 Fraedrich, K., Gerstengarbe, F.W., Werner, P.C., 2001. Climate shifts during the last century. *Clim. Change*, 50(4): 405-417.
522 <https://doi.org/10.1023/a:1010699428863>

523 Gao, G.Y., Fu, B.J., Wang, S., Liang, W., Jiang, X.H., 2016a. Determining the hydrological responses to climate variability and land
524 use/cover change in the Loess Plateau with the Budyko framework. *Sci. Total Environ.*, 557-558: 331-42.
525 <https://doi.org/10.1016/j.scitotenv.2016.03.019>

526 Gao, P., Jiang, G., Wei, Y., Mu, X., Wang, F., Zhao, G., Sun, W., 2015. Streamflow regimes of the Yanhe River under climate and land
527 use change, Loess Plateau, China. *Hydrol. Process.*, 29(10): 2402-2413. <https://doi.org/10.1002/hyp.10309>

528 Gao, P., Geissen, V., Ritsema, C.J., Mu, X.M., Wang, F., 2013. Impact of climate change and anthropogenic activities on stream flow
529 and sediment discharge in the Wei River basin, China. *Hydrol. Earth Syst. Sci.*, 17(3): 961-972. <https://doi.org/10.5194/hess-17-961-2013>

530 961-2013

531 Gao, Z., Zhang, L., Zhang, X., Cheng, L., Potter, N., Cowan, T., Cai, W., 2016b. Long-term streamflow trends in the middle reaches of
532 the Yellow River Basin: detecting drivers of change. *Hydrol. Process.*, 30(9): 1315-1329. <https://doi.org/10.1002/hyp.10704>

533 Grossmann, A., Kronland-Martinet, R., Morlet, J., 1990. Reading and Understanding Continuous Wavelet Transforms. *Wavelets.*
534 Springer Berlin Heidelberg, Berlin, Heidelberg, pp. 2-20.

535 Guo, Y., Li, Z.J., Amo-Boateng, M., Deng, P., Huang, P.N., 2013. Quantitative assessment of the impact of climate variability and human
536 activities on runoff changes for the upper reaches of Weihe River. *Stoch. Environ. Res. Risk Assess.*, 28(2): 333-346.
537 <https://doi.org/10.1007/s00477-013-0752-8>

538 Hamed, K.H., 2008. Trend detection in hydrologic data: The Mann–Kendall trend test under the scaling hypothesis. *J. Hydrol.*, 349(3):

539 350-363. <https://doi.org/10.1016/j.jhydrol.2007.11.009>

540 Hamed, K.H., Rao, A.R., 1998. A modified Mann-Kendall trend test for autocorrelated data. *J. Hydrol.*, 204(1-4): 182-196.
541 [https://doi.org/10.1016/s0022-1694\(97\)00125-x](https://doi.org/10.1016/s0022-1694(97)00125-x)

542 Hao, Y., Liu, G., Li, H., Li, Z., Zhao, J., J. Yeh, T.C., 2012. Investigation of karstic hydrological processes of Niangziguan Springs (North
543 China) using wavelet analysis. *Hydrol. Process.*, 26(20): 3062-3069. <https://doi.org/10.1002/hyp.8265>

544 Hosking, J.R.M., 1984. Modeling persistence in hydrological time series using fractional differencing. *Water Resour. Res.*, 20(12): 1898-
545 1908. <https://doi.org/10.1029/WR020i012p01898>

546 Huang, N.E., Shen, Z., Long, S.R., Wu, M.C., Shih, H.H., Zheng, Q., Yen, N.C., Tung, C.C., Liu, H.H., 1998. The empirical mode
547 decomposition and the Hilbert spectrum for nonlinear and non-stationary time series analysis, *Proc. Math. Phys. Eng. Sci. The*
548 *Royal Society*, pp. 903-995. <https://doi.org/10.1098/rspa.1998.0193>

549 Huang, S., Liu, D., Huang, Q., Chen, Y., 2016. Contributions of climate variability and human activities to the variation of runoff in the
550 Wei River Basin, China. *Hydrolog. Sci. J.*, 61(6): 1026-1039. DOI:10.1080/02626667.2014.959955

551 Huang, S.Z., Huang, Q., Leng, G.Y., Zhao, M.L., Meng, E., 2017. Variations in annual water-energy balance and their correlations with
552 vegetation and soil moisture dynamics: A case study in the Wei River Basin, China. *J. Hydrol.*, 546: 515-525.
553 <https://doi.org/10.1016/j.jhydrol.2016.12.060>

554 Ishak, E.H., Rahman, A., Westra, S., Sharma, A., Kuczera, G., 2013. Evaluating the non-stationarity of Australian annual maximum
555 flood. *J. Hydrol.*, 494: 134-145. <https://doi.org/10.1016/j.jhydrol.2013.04.021>

556 Islamoglu, Y., 2003. A new approach for the prediction of the heat transfer rate of the wire-on-tube type heat exchanger—use of an
557 artificial neural network model. *Appl. Therm. Eng.*, 23(2): 243-249. [https://doi.org/10.1016/S1359-4311\(02\)00155-2](https://doi.org/10.1016/S1359-4311(02)00155-2)

558 Jenouvrier, S., Barbraud, C., Cazelles, B., Weimerskirch, H., 2005. Modelling population dynamics of seabirds: importance of the effects
559 of climate fluctuations on breeding proportions. *Oikos*, 108(3): 511-522. <https://doi.org/10.1111/j.0030-1299.2005.13351.x>

560 Jiang, C., Xiong, L., Wang, D., Liu, P., Guo, S., Xu, C.Y., 2015. Separating the impacts of climate change and human activities on runoff
561 using the Budyko-type equations with time-varying parameters. *J. Hydrol.*, 522: 326-338.
562 <https://doi.org/10.1016/j.jhydrol.2014.12.060>

563 Kam, J.H., Sheffield, J., 2016. Changes in the low flow regime over the eastern United States (1962–2011): variability, trends, and
564 attributions. *J. Hydrol.*, 135(3-4): 639-653. <https://doi.org/10.1007/s10584-015-1574-0>

565 Karthikeyan, L., Nagesh Kumar, D., 2013. Predictability of nonstationary time series using wavelet and EMD based ARMA models. *J.*
566 *Hydrol.*, 502: 103-119. <https://doi.org/10.1016/j.jhydrol.2013.08.030>

567 Kendall, M.G., 1975. *Rank Correlation Methods*. Charles Griffin, London. [https://doi.org/S0022-1694\(14\)00179-6/h0205](https://doi.org/S0022-1694(14)00179-6/h0205)

568 Koch, F., Prasad, M., Bach, H., Mauser, W., Appel, F., Weber, M., 2011. How Will Hydroelectric Power Generation Develop under
569 Climate Change Scenarios? A Case Study in the Upper Danube Basin. *Energies*, 4(10): 1508. <https://doi.org/10.3390/en4101508>

570 Kutner, M.H., Nachtsheim, C.J., Neter, J., Li, W., 2005. *Applied linear statistical models*, 5. McGraw-Hill Irwin Boston.

571 Labat, D., 2005. Recent advances in wavelet analyses: Part 1. A review of concepts. *J. Hydrol.*, 314(1-4): 275-288.
572 <https://doi.org/10.1016/j.jhydrol.2005.04.003>

573 Labat, D., 2010. Cross wavelet analyses of annual continental freshwater discharge and selected climate indices. *J. Hydrol.*, 385(1): 269-
574 278. <https://doi.org/10.1016/j.jhydrol.2010.02.029>

575 Labat, D., Ababou, R., Mangin, A., 2000. Rainfall–runoff relations for karstic springs. Part II: continuous wavelet and discrete orthogonal
576 multiresolution analyses. *J. Hydrol.*, 238(3): 149-178. [https://doi.org/10.1016/s0022-1694\(00\)00322-x](https://doi.org/10.1016/s0022-1694(00)00322-x)

577 Lang, M., Ouarda, T.B.M.J., Bobée, B., 1999. Towards operational guidelines for over-threshold modeling. *J. Hydrol.*, 225(3): 103-117.
578 [https://doi.org/10.1016/s0022-1694\(99\)00167-5](https://doi.org/10.1016/s0022-1694(99)00167-5)

579 Li, H.J., Gao, J.E., Zhang, H.C., Zhang, Y.X., Zhang, Y.Y., 2017. Response of extreme precipitation to Solar activity and El Nino events
580 in typical regions of the Loess Plateau. *Adv. Meteorol.*, 2017: 1-9. <https://doi.org/10.1155/2017/9823865>

581 Li, M., Xia, J., Chen, Z., Meng, D., Xu, C., 2013. Variation analysis of precipitation during past 286 years in Beijing area, China, using
582 non-parametric test and wavelet analysis. *Hydrol. Process.*, 27(20): 2934-2943. <https://doi.org/10.1002/hyp.9388>

583 Li, Y., Chang, J., Luo, L., Wang, Y., Guo, A., Ma, F., Fan, J., 2019. Spatiotemporal impacts of land use land cover changes on hydrology
584 from the mechanism perspective using SWAT model with time-varying parameters. *Hydrol. Res.*, 50(1): 244-261.
585 <https://doi.org/10.2166/nh.2018.006>

586 Lin, J., Qu, L., 2000. Feature extraction based on Morlet wavelet and its application for mechanical fault diagnosis. *J. Sound Vib.*, 234(1):
587 135-148. DOI:<https://doi.org/10.1006/jsvi.2000.2864>

588 Lv, J.Q., Bing, S., Shao, N.H., Dong, K.P., Li, K.B., 2012. Evolution modes and EMD gray self-memory model of the Yellow River
589 water resources. *J. Hydroelectric Eng.*, 31(3): 25-30. (in Chinese)

590 Machiwal, D., Kumar, S., Dayal, D., Mangalassery, S., 2017. Identifying abrupt changes and detecting gradual trends of annual rainfall
591 in an Indian arid region under heightened rainfall rise regime. *Int. J. Climatol.*, 37(5): 2719-2733. <https://doi.org/10.1002/joc.4875>

592 Mann, H.B., 1945. Nonparametric Tests Against Trend. *Econometrica*, 13(3): 245-259. <https://doi.org/10.2307/1907187>

593 Matalas, N.C., 1967. Time series analysis. *Water Resour. Res.*, 3(3): 817-829. <https://doi.org/10.1029/WR003i003p00817>

594 Méndez, F.J., Menéndez, M., Luceño, A., Losada, I.J., 2006. Estimation of the long-term variability of extreme significant wave height
595 using a time-dependent Peak Over Threshold (POT) model. *J. Geophys. Res. Oceans*, 111(C7).
596 <https://doi.org/10.1029/2005jc003344>

597 Milly, P.C.D., Wetherald, R.T., Dunne, K.A., Delworth, T.L., 2002. Increasing risk of great floods in a changing climate. *Nature*, 415:
598 514. <https://doi.org/10.1038/415514a>

599 Mohammadkarimi, M., Dobre, O.A., 2014. Blind Identification of Spatial Multiplexing and Alamouti Space-Time Block Code via
600 Kolmogorov-Smirnov (K-S) Test. *IEEE Commun. Lett.*, 18(10): 1711-1714. <https://doi.org/10.1109/LCOMM.2014.2352305>

601 Morlet, J., Arens, G., Fourgeau, E., Glard, D., 1982. Wave propagation and sampling theory—Part I: Complex signal and scattering in
602 multilayered media. *Geophysics*, 47(2): 203-221. <https://doi.org/10.1190/1.1441328>

603 Nakken, M., 1999. Wavelet analysis of rainfall–runoff variability isolating climatic from anthropogenic patterns. *Environ. Modell. Softw.*,
604 14(4): 283-295. [https://doi.org/10.1016/S1364-8152\(98\)00080-2](https://doi.org/10.1016/S1364-8152(98)00080-2)

605 Nash, J.E., Sutcliffe, J.V., 1970. River flow forecasting through conceptual models part I — A discussion of principles. *J. Hydrol.*, 10(3):
606 282-290. [https://doi.org/10.1016/0022-1694\(70\)90255-6](https://doi.org/10.1016/0022-1694(70)90255-6)

607 Okabe, A., Boots, B., Sugihara, K., Chiu, S.N., 2009. Spatial tessellations: concepts and applications of Voronoi diagrams, 501. John
608 Wiley & Sons.

609 Onuki, Y., Ohshima, K., Kaseda, C., Arai, H., Suzuki, T., Takayama, K., 2008. Evaluation of the reliability of nonlinear optimal solutions
610 in pharmaceuticals using a bootstrap resampling technique in combination with Kohonen's self-organizing maps. *J. Pharm. SCI-*
611 *US.*, 97(1): 331-339. <https://doi.org/10.1002/jps.21097>

612 Partovian, A., Nourani, V., Alami, M.T., 2016. Hybrid denoising-jittering data processing approach to enhance sediment load prediction
613 of muddy rivers. *J. Mt. Sci.*, 13(12): 2135-2146. <https://doi.org/10.1007/s11629-016-3884-8>

614 Pettitt, A.N., 1979. A non-parametric approach to the change-point problem. *Appl. Stat.*, 28(2): 126-135. <https://doi.org/10.2307/2346729>

615 Reeves, J., Chen, J., Wang, X.L.L., Lund, R., Lu, Q.Q., 2007. A review and comparison of changepoint detection techniques for climate
616 data. *J. Appl. Meteorol. Climatol.*, 46(6): 900-915. <https://doi.org/10.1175/jam2493.1>

617 Rougé, C., Ge, Y., Cai, X.M., 2013. Detecting gradual and abrupt changes in hydrological records. *Adv. Water Resour.*, 53: 33-44.
618 <https://doi.org/10.1016/j.advwatres.2012.09.008>

619 Salas, J.D., 1980. Applied modeling of hydrologic time series. Water Resources Publication.

620 Serinaldi, F., Kilsby, C.G., 2016. The importance of prewhitening in change point analysis under persistence. *Stoch. Environ. Res. Risk*
621 *Assess.*, 30(2): 763-777. <https://doi.org/10.1007/s00477-015-1041-5>

622 Serinaldi, F., Kilsby, C.G., Lombardo, F., 2018. Untenable nonstationarity: An assessment of the fitness for purpose of trend tests in

623 hydrology. *Adv. Water Resour.*, 111: 132-155. <https://doi.org/10.1016/j.advwatres.2017.10.015>

624 Stojković, M., Ilić, A., Prohaska, S., Plavšić, J., 2014. Multi-Temporal Analysis of Mean Annual and Seasonal Stream Flow Trends,
625 Including Periodicity and Multiple Non-Linear Regression. *Water Resour. Manag.*, 28(12): 4319-4335.
626 <https://doi.org/10.1007/s11269-014-0753-5>

627 Tan, M.L., Ficklin, D.L., Dixon, B., Ibrahim, A.L., Yusop, Z., Chaplot, V., 2015. Impacts of DEM resolution, source, and resampling
628 technique on SWAT-simulated streamflow. *Applied Geography*, 63: 357-368. <https://doi.org/10.1016/j.apgeog.2015.07.014>

629 Tokar, A.S., Johnson, P.A., 1999. Rainfall-runoff modeling using artificial neural networks. *J. Hydrol. Eng.*, 4(3): 232-239.
630 <https://doi.org/10.1061/%2F%28asce%291084-0699%282001%296%3A2%28176%29>

631 Torrence, C., Compo, G.P., 1998. A practical guide to wavelet analysis. *Bulletin of the American Meteorological society*, 79(1): 61-78.

632 Troy, T.J., Pavao-Zuckerman, M., Evans, T.P., 2015. Debates—Perspectives on socio-hydrology: Socio-hydrologic modeling: Tradeoffs,
633 hypothesis testing, and validation. *Water Resour. Res.*, 51(6): 4806-4814. <https://doi.org/10.1002/2015WR017046>

634 Verbesselt, J., Hyndman, R., Zeileis, A., Culvenor, D., 2010. Phenological change detection while accounting for abrupt and gradual
635 trends in satellite image time series. *Remote Sens. Environ.*, 114(12): 2970-2980. <https://doi.org/10.1016/j.rse.2010.08.003>

636 Wang, F., Hessel, R., Mu, X., Maroulis, J., Zhao, G., Geissen, V., Ritsema, C., 2015. Distinguishing the impacts of human activities and
637 climate variability on runoff and sediment load change based on paired periods with similar weather conditions: A case in the Yan
638 River, China. *J. Hydrol.*, 527: 884-893. <https://doi.org/10.1016/j.jhydrol.2015.05.037>

639 Wang, X., 2014. Advances in separating effects of climate variability and human activity on stream discharge: An overview. *Adv. Water
640 Resour.*, 71: 209-218. <https://doi.org/10.1016/j.advwatres.2014.06.007>

641 Wei, F.Y., Cao, H.X., 1993. A fuzzy mean generating function (FMGF) model and its application. *Meteorol. Mon.*, 2: 7-11. (in Chinese)

642 Wei, P., Zheng, J.Y., Xiao, L.B., Yan, F.F., 2013. The relationship of nature runoff changes in flood-season of middle Yellow River and
643 Yongding River, 1766-2004. *Acta. Geogr. Sin.*, 68(7): 975-982. (in Chinese)

644 Wei, Y., Jiao, J., Zhao, G., Zhao, H., He, Z., Mu, X., 2016. Spatial - temporal variation and periodic change in streamflow and suspended
645 sediment discharge along the mainstream of the Yellow River during 1950 - 2013. *Catena*, 140: 105-115.
646 <https://doi.org/10.1016/j.catena.2016.01.016>

647 Werner, R., 2008. The latitudinal ozone variability study using wavelet analysis. *J. Atmos. Sol. Terr. Phys.*, 70(2-4): 261-267.
648 <https://doi.org/10.1016/j.jastp.2007.08.022>

649 White, M.A., Schmidt, J.C., Topping, D.J., 2005. Application of wavelet analysis for monitoring the hydrologic effects of dam operation:
650 Glen Canyon Dam and the Colorado River at Lees Ferry, Arizona. *River Res. Appl.*, 21(5): 551-565. <https://doi.org/10.1002/rra.827>

651 Wu, H.S., Liu, D.F., Chang, J.X., Zhang, H.X., Huang, Q., 2017a. Impacts of climate change and human activities on runoff in Weihe
652 Basin based on Budyko hypothesis. *IOP Conference Series: Earth Env. Sci.*, 82: 012063. DOI:10.1088/1755-1315/82/1/012063

653 Wu, J., Chen, Y., Hang, Q., 2016. Analysis of Inconsistent Hydrological Frequency Based on TFPW-MK-Pettitt and EEMD,
654 Environmental Science and Sustainable Development: International Conference on Environmental Science and Sustainable
655 Development (ICESSD 2015). World Scientific, pp. 198-207.

656 Wu, J.W., Miao, C.Y., Zhang, X.M., Yang, T.T., Duan, Q.Y., 2017b. Detecting the quantitative hydrological response to changes in
657 climate and human activities. *Sci. Total Environ.*, 586: 328-337. <https://doi.org/10.1016/j.scitotenv.2017.02.010>

658 Wu, L., Long, T.Y., Liu, X., Guo, J.S., 2012. Impacts of climate and land-use changes on the migration of non-point source nitrogen and
659 phosphorus during rainfall-runoff in the Jialing River Watershed, China. *J. Hydrol.*, 475: 26-41.
660 <https://doi.org/10.1016/j.jhydrol.2012.08.022>

661 Wu, L., Wang, S., Bai, X., Luo, W., Tian, Y., Zeng, C., Luo, G., He, S., 2017c. Quantitative assessment of the impacts of climate change
662 and human activities on runoff change in a typical karst watershed, SW China. *Sci. Total Environ.*, 601-602: 1449-1465.
663 <https://doi.org/10.1016/j.scitotenv.2017.05.288>

664 Wu, Z., Huang, N.E., 2009. Ensemble Empirical Mode Decomposition: A Noise-assisted data analysis method. *Advances in Adaptive*

665 Data Analysis, 01(01): 1-41. DOI:10.1142/s1793536909000047

666 Yuan, F., Berndtsson, R., Zhang, L., Uvo, C. B., Hao, Z., Wang, X., Yasuda, H., 2015. Hydro climatic trend and periodicity for the source
667 region of the Yellow River. *J. Hydrol. Eng.*, 20(10): 05015003. [https://doi.org/10.1061/\(asce\)he.1943-5584.0001182](https://doi.org/10.1061/(asce)he.1943-5584.0001182)

668 Yuan, F., Yasuda, H., Berndtsson, R., Bertacchi Uvo, C., Zhang, L., Hao, Z., Wang, X., 2016. Regional sea-surface temperatures explain
669 spatial and temporal variation of summer precipitation in the source region of the Yellow River. *Hydrolog. Sci. J.*, 61(8): 1383-1394.
670 <https://doi.org/10.1080/02626667.2015.1035658>

671 Yue, S., Pilon, P., Cavadias, G., 2002a. Power of the Mann–Kendall and Spearman's rho tests for detecting monotonic trends in
672 hydrological series. *J. Hydrol.*, 259(1-4): 254-271. [https://doi.org/10.1016/s0022-1694\(01\)00594-7](https://doi.org/10.1016/s0022-1694(01)00594-7)

673 Yue, S., Pilon, P., Phinney, B., 2003. Canadian streamflow trend detection: impacts of serial and cross-correlation. *Hydrolog. Sci. J.*,
674 48(1): 51-63. <https://doi.org/10.1623/hysj.48.1.51.43478>

675 Yue, S., Pilon, P., Phinney, B., Cavadias, G., 2002b. The influence of autocorrelation on the ability to detect trend in hydrological series.
676 *Hydrol. Process.*, 16(9): 1807-1829. <https://doi.org/10.1002/hyp.1095>

677 Yue, S., Wang, C.Y., 2004. The Mann-Kendall test modified by effective sample size to detect trend in serially correlated hydrological
678 series. *Water Resour. Manag.*, 18(3): 201-218. <https://doi.org/10.1023/b:warm.0000043140.61082.60>

679 Zhai, R., Tao, F.L., 2017. Contributions of climate change and human activities to runoff change in seven typical catchments across
680 China. *Sci. Total Environ.*, 605-606: 219-229. <https://doi.org/10.1016/j.scitotenv.2017.06.210>

681 Zhan, C.S., Jiang, S.S., Sun, F.B., Jia, Y.W., Niu, C.W., Yue, W.F., 2014. Quantitative contribution of climate change and human activities
682 to runoff changes in the Wei River basin, China. *Hydrol. Earth Syst. Sci.*, 18(8): 3069-3077. [https://doi.org/10.5194/hess-18-3069-](https://doi.org/10.5194/hess-18-3069-2014)
683 2014

684 Zhang, A., Zhang, C., Fu, G., Wang, B., Bao, Z., Zheng, H., 2012. Assessments of impacts of climate change and human activities on
685 runoff with SWAT for the Huifa River Basin, Northeast China. *Water Resour. Manag.*, 26(8): 2199-2217.
686 <https://doi.org/10.1007/s11269-012-0010-8>

687 Zhang, A.J., Zheng, C.M., Wang, S., Yao, Y.Y., 2015. Analysis of streamflow variations in the Heihe River Basin, northwest China:
688 trends, abrupt changes, driving factors and ecological influences. *J. Hydrol.*, 3: 106-124. <https://doi.org/10.1016/j.ejrh.2014.10.005>

689 Zhang, H., Huang, Q., Zhang, Q., Gu, L., Chen, K., Yu, Q., 2016. Changes in the long-term hydrological regimes and the impacts of
690 human activities in the main Wei River, China. *Hydrolog. Sci. J.*, 61(6): 1054-1068.
691 <https://doi.org/10.1080/02626667.2015.1027708>

692 Zhang, Q., Chen, J., Becker, S., 2007. Flood/drought change of last millennium in the Yangtze Delta and its possible connections with
693 Tibetan climatic changes. *Global Planet. Change*, 57(3): 213-221. <https://doi.org/10.1016/j.gloplacha.2006.11.010>

694 Zhang, Q., Singh, V.P., Li, K., Li, J., 2014. Trend, periodicity and abrupt change in streamflow of the East River, the Pearl River basin.
695 *Hydrol. Process.*, 28(2): 305-314. <https://doi.org/10.1002/hyp.9576>

696 Zhao, G., Mu, X., Jiao, J., An, Z., Klik, A., Wang, F., Jiao, F., Yue, X., Gao, P., Sun, W., 2017. Evidence and causes of spatiotemporal
697 changes in runoff and sediment yield on the Chinese Loess Plateau. *Land Degrad. Dev.*, 28(2): 579-590.
698 <https://doi.org/10.1002/ldr.2534>

699 Zhao, G.J., Mu, X.M., Tian, P., Wang, F., Gao, P., 2013. Climate changes and their impacts on water resources in semiarid regions: a
700 case study of the Wei River basin, China. *Hydrol. Process.*, 27(26): 3852-3863. <https://doi.org/10.1002/hyp.9504>

701 Zhao, J., Huang, Q., Chang, J., Liu, D., Huang, S., Shi, X., 2015. Analysis of temporal and spatial trends of hydro-climatic variables in
702 the Wei River Basin. *Environ. Res.*, 139: 55-64. <https://doi.org/10.1016/j.envres.2014.12.028>

703 Zou, L., Xia, J., She, D., 2018. Analysis of Impacts of Climate Change and Human Activities on Hydrological Drought: a Case Study in
704 the Wei River Basin, China. *Water Resour. Manag.*, 32(4): 1421-1438. DOI:10.1007/s11269-017-1877-1

705 Zuo, D., Xu, Z., Yao, W., Jin, S., Xiao, P., Ran, D., 2016. Assessing the effects of changes in land use and climate on runoff and sediment
706 yields from a watershed in the Loess Plateau of China. *Sci. Total Environ.*, 544: 238-250.

- 707 <https://doi.org/10.1016/j.scitotenv.2015.11.060>
- 708 Zuo, D.P., Xu, Z.X., Yang, H., Liu, X.C., 2012. Spatiotemporal variations and abrupt changes of potential evapotranspiration and its
709 sensitivity to key meteorological variables in the Wei River basin, China. *Hydrol. Process.*, 26(8): 1149-1160.
710 <https://doi.org/10.1002/hyp.8206>
- 711 Zuo, D.P., Xu, Z.X., Zhao, J., Abbaspour, K.C., Yang, H., 2015. Response of runoff to climate change in the Wei River basin, China.
712 *Hydrolog. Sci. J.*, 60(3): 508-522. <https://doi.org/10.1080/02626667.2014.943668>
- 713 Zuo, Q.T., Gao, F., 2004. Periodic overlap prediction model and its three improved models of hydrological time series. *J. Zhengzhou*
714 *Univ. (Sci. Eng.)*, 25(4): 67-73. (in Chinese)

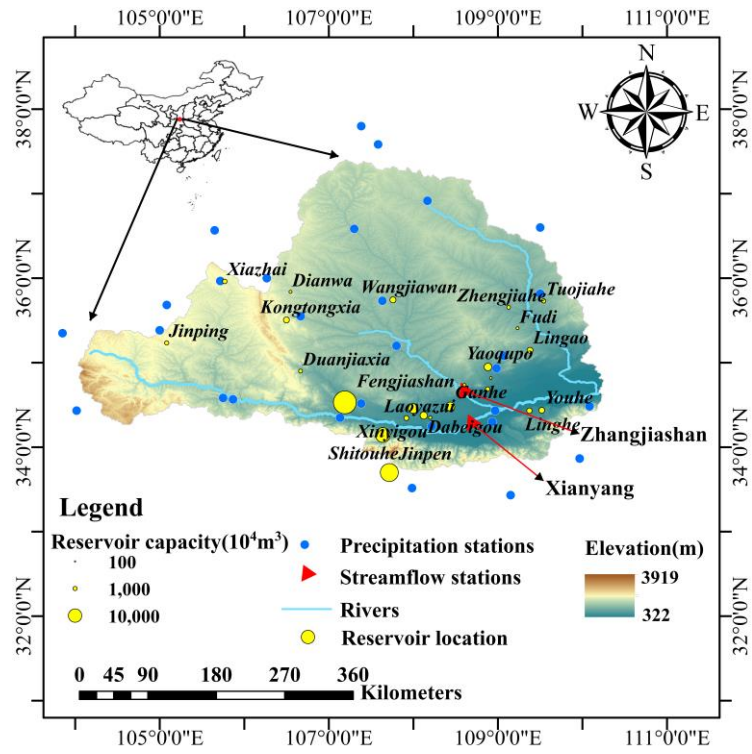


Figure 1. Locations of precipitation stations, hydrological gauges and main reservoirs in the Wei River basin, China.

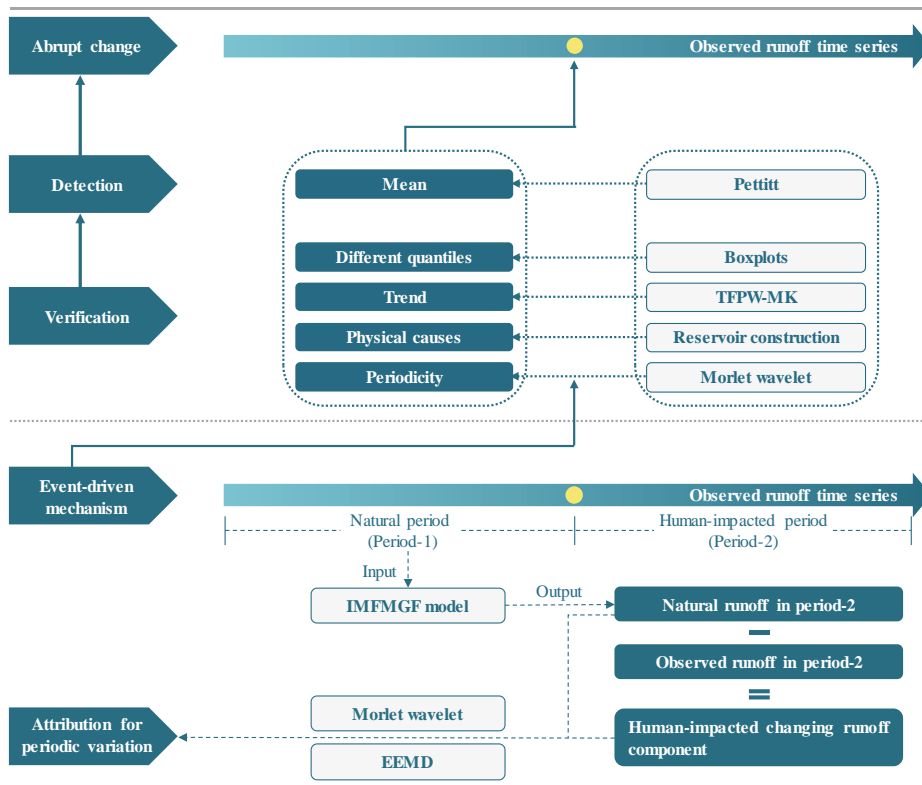


Figure 2. Flowchart for methodologies of detection and attribution of abrupt shift of periodicity in long-term runoff series.

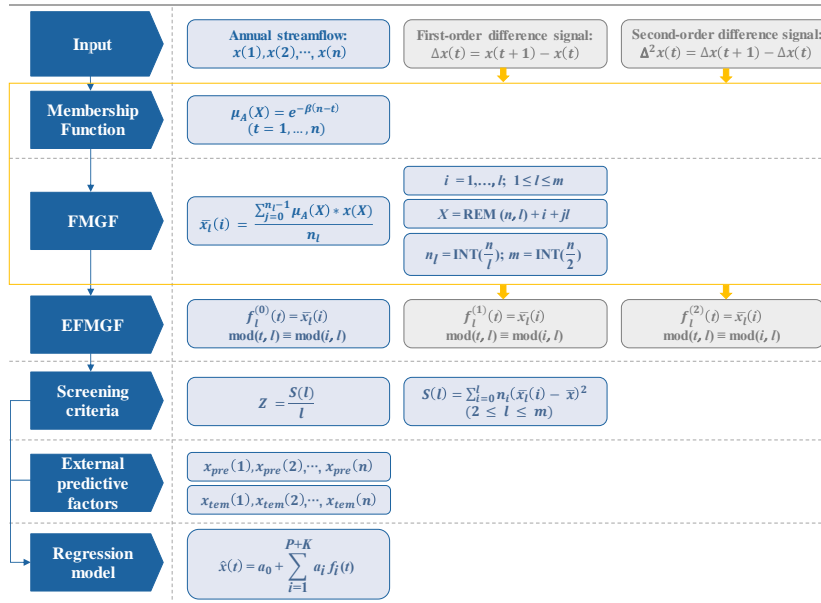
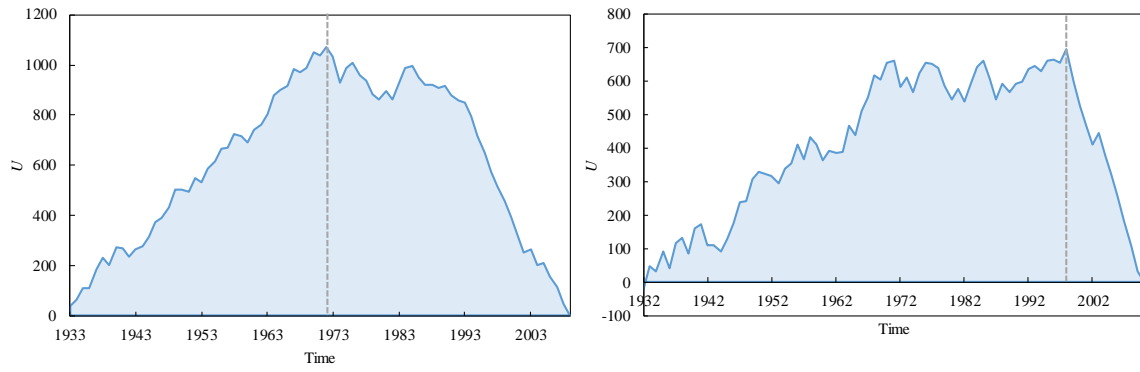


Figure 3. Calculation by the Improved Multivariate Fuzzy Mean Generating Function (IMFMGF) forecast model.



(a)

(b)

Figure 4. The results of Pettitt test at Xianyang gauge (a) and Zhangjiashan gauge (b). U denotes the Mann and Whitney statistical value. The most significantly abrupt point is where U is the largest values.

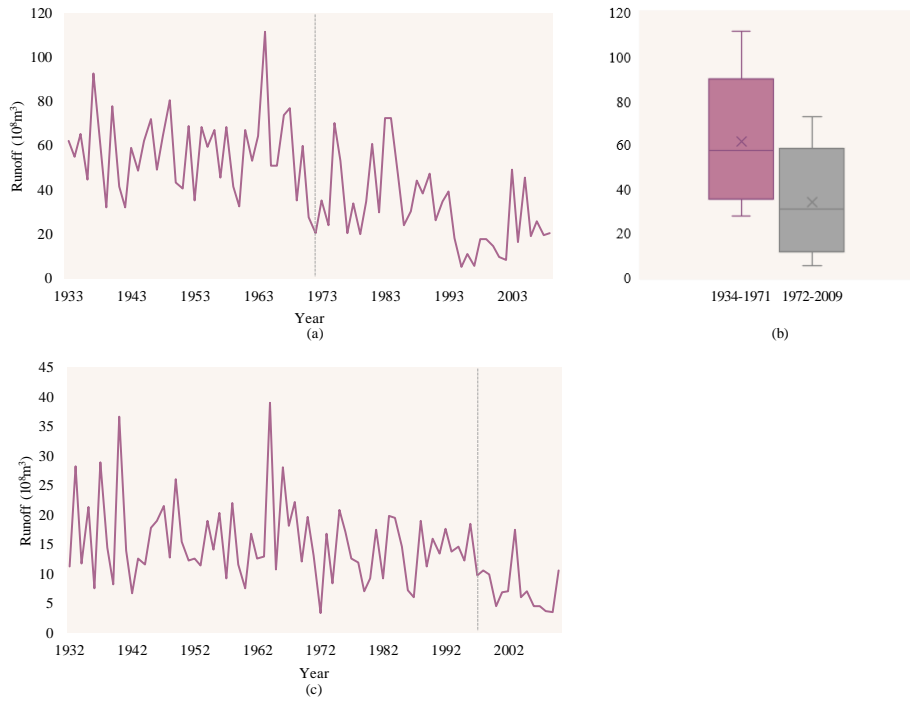
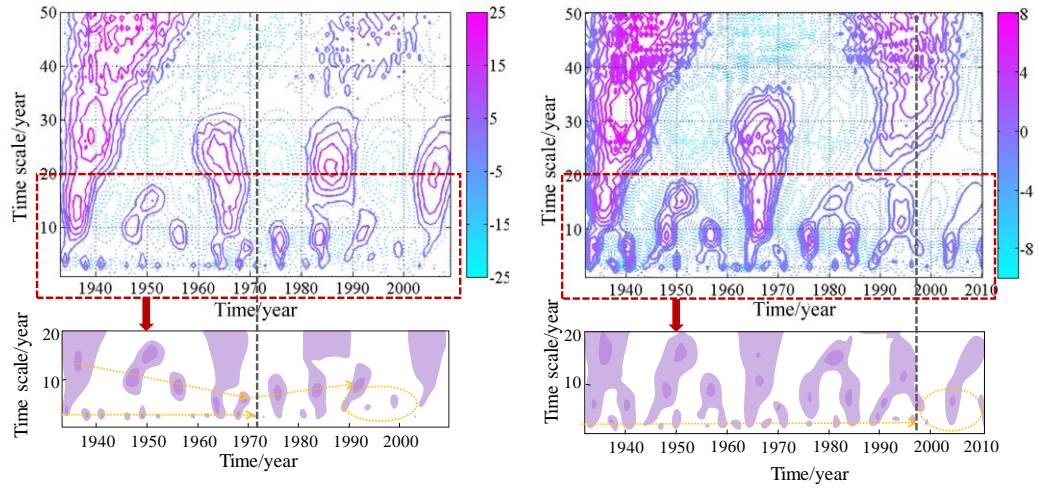


Figure 5. The annual runoff at Xianyang gauge in 1933-2009 (a) and the boxplots for the characteristics of its sub-sections (b); the annual runoff at Zhangjiashan gauge in 1932-2010 (c).



(a)

(b)

Figure 6. Real part of the wavelet coefficient contour maps of the observed runoff and their schematics in minor periods at Xianyang gauge (a) and Zhangjiashan gauge (b).

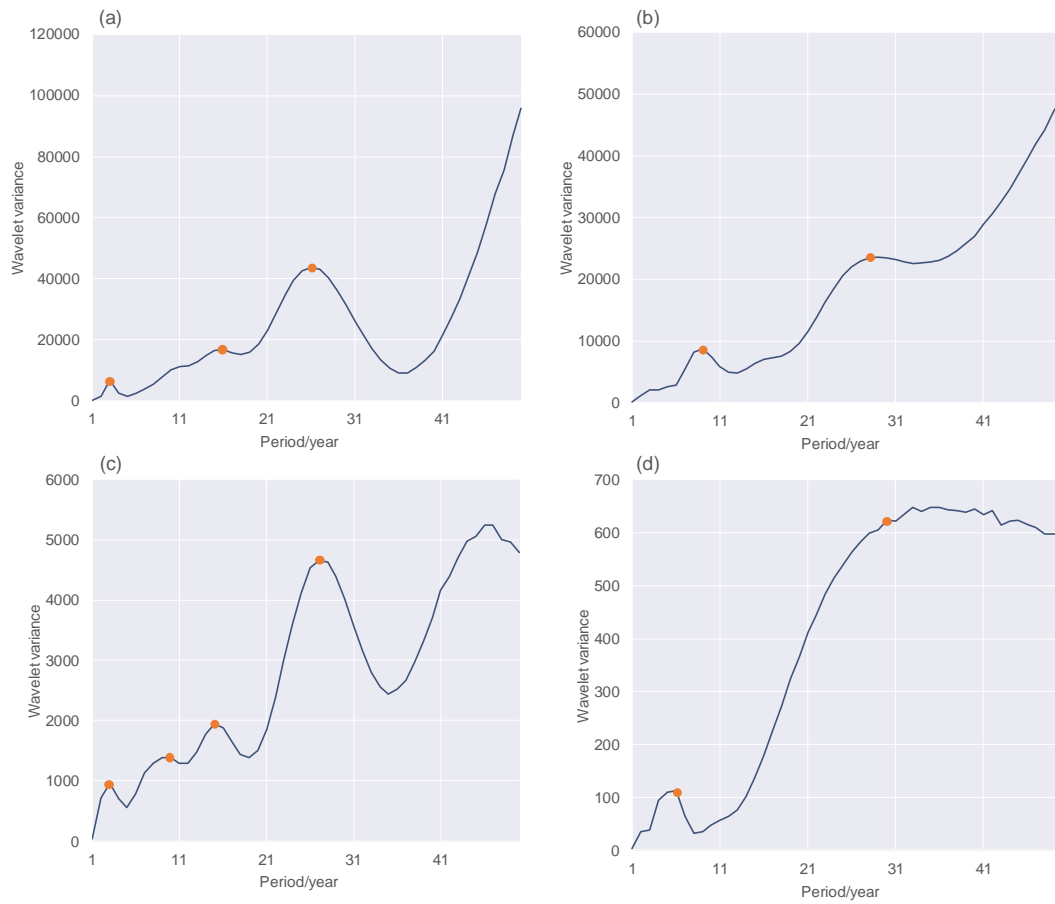


Figure 7. (a): Wavelet variance for the observed runoff before the abrupt change point at Xianyang gauge; **(b):** Wavelet variance for the observed runoff after the abrupt change point at Xianyang gauge; **(c):** Wavelet variance for the observed runoff before the abrupt change point at Zhangjiashan gauge; **(d):** Wavelet variance for the observed runoff after the abrupt change point at Zhangjiashan gauge. The red points denote the major periods of the runoff time series which were identified by Morlet wavelet analysis.

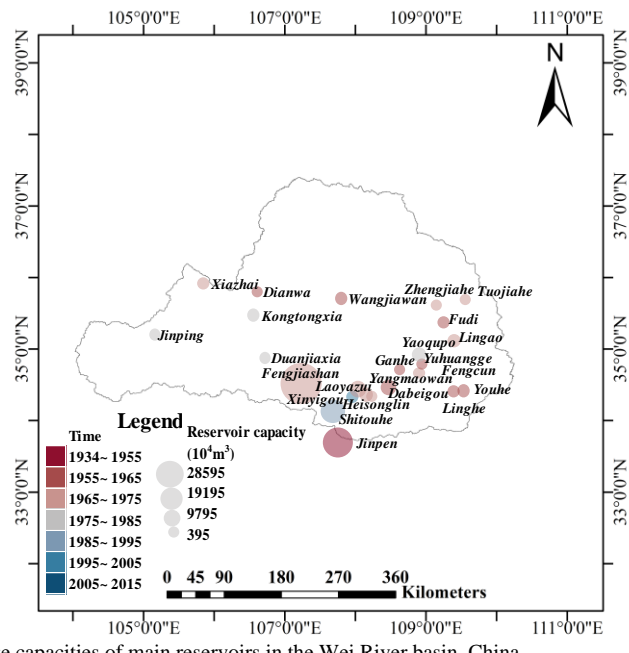


Figure 8. Completion time and storage capacities of main reservoirs in the Wei River basin, China.

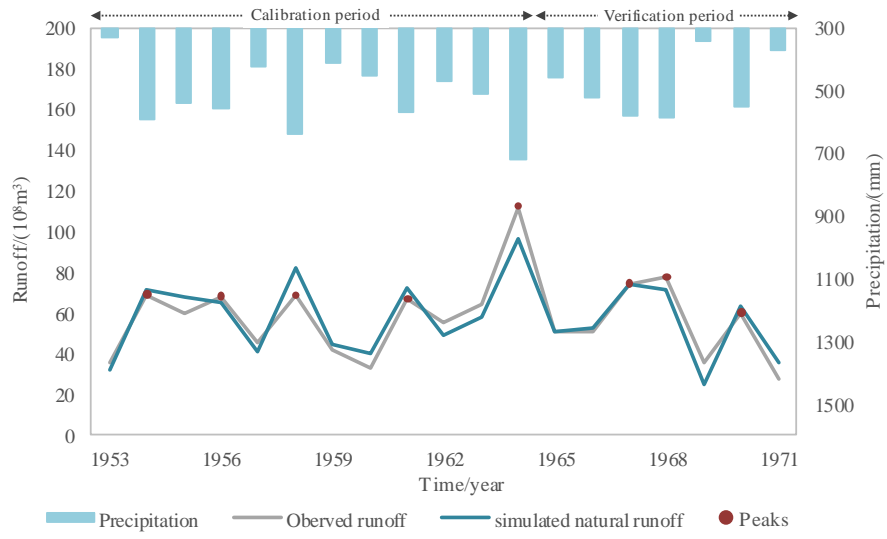


Figure 9. The observed runoff and simulated natural runoff in 1953-1971 at Xianyang gauge.

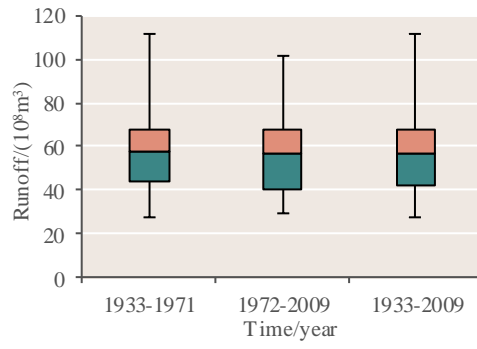


Figure 10. The boxplots of the natural runoff in 1933-1971, 1972-2009 and 1933-2009 at Xianyang gauge. The natural runoff is the observed natural runoff in 1933-1971 and the simulated natural runoff in 1972-2009.

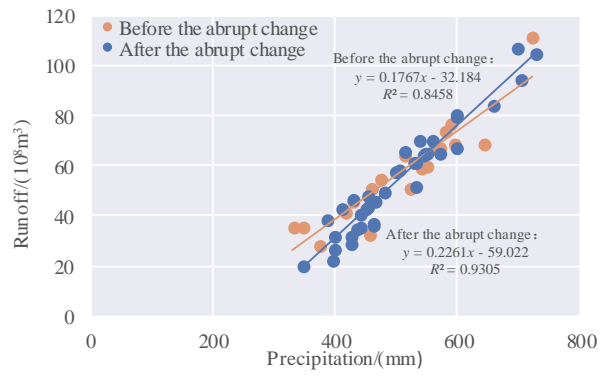


Figure 11. The precipitation-measured runoff relationships before the abrupt change (1971) and the precipitation-simulated natural runoff relationships after the abrupt change at Xianyang gauge.

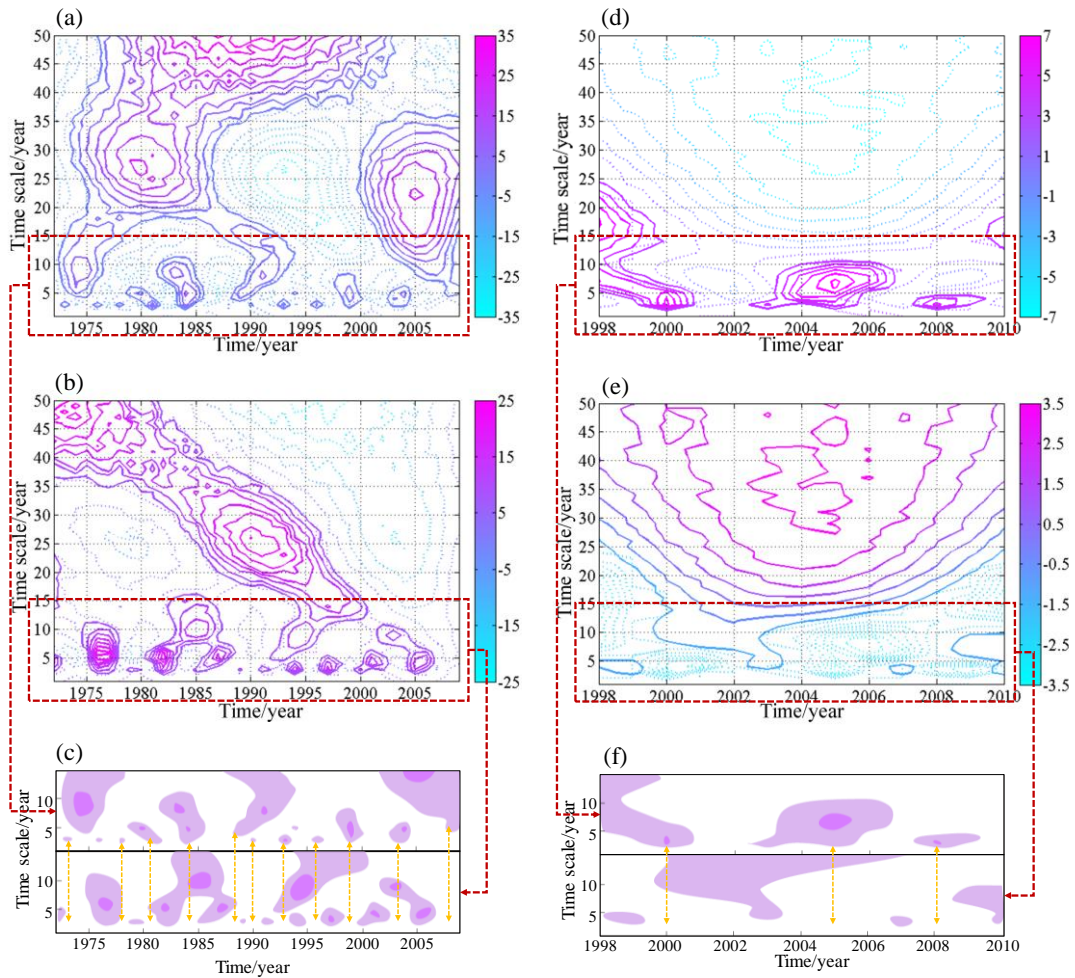


Figure 12. (a): Real part contour maps of wavelet coefficients of natural runoff components in period-2 (human-impacted period) at Xianyang gauge; (b): real part contour maps of wavelet coefficients of human-impacted runoff components in period-2 at Xianyang gauge; (c): the schematics of Figure 12 (a) and Figure 12 (b) in minor periods at Xianyang gauge; (d): Real part contour maps of wavelet coefficients of natural runoff components in period-2 at Zhangjiashan gauge; (e): real part contour maps of wavelet coefficients of human-impacted runoff components in period-2 at Zhangjiashan gauge; (f): the schematics of Figure 12 (d) and Figure 12 (e) in minor periods at Zhangjiashan gauge. According to the schematics in their minor periods, it is interesting to note that the wave crests and troughs of the two components in 3-4-year minor periods have good negative correspondence. Specifically, when the minor periods of natural component series are in the troughs, the minor periods of human-impacted runoff component series are at the peaks, and vice versa.

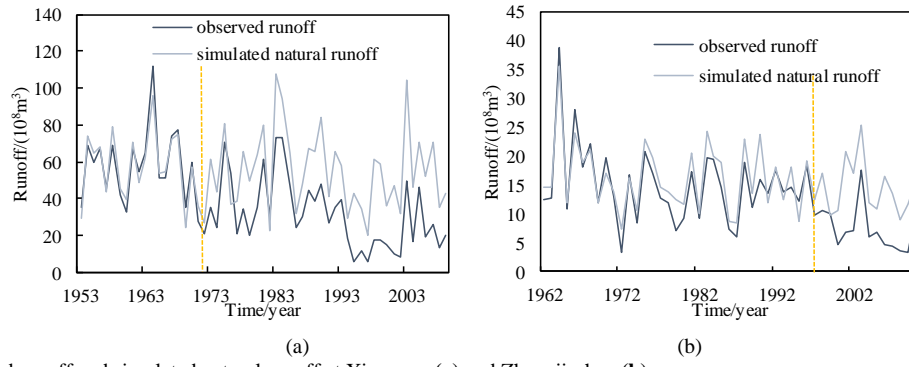


Figure 13. Observed runoff and simulated natural runoff at Xianyang (a) and Zhangjiashan (b) gauges.

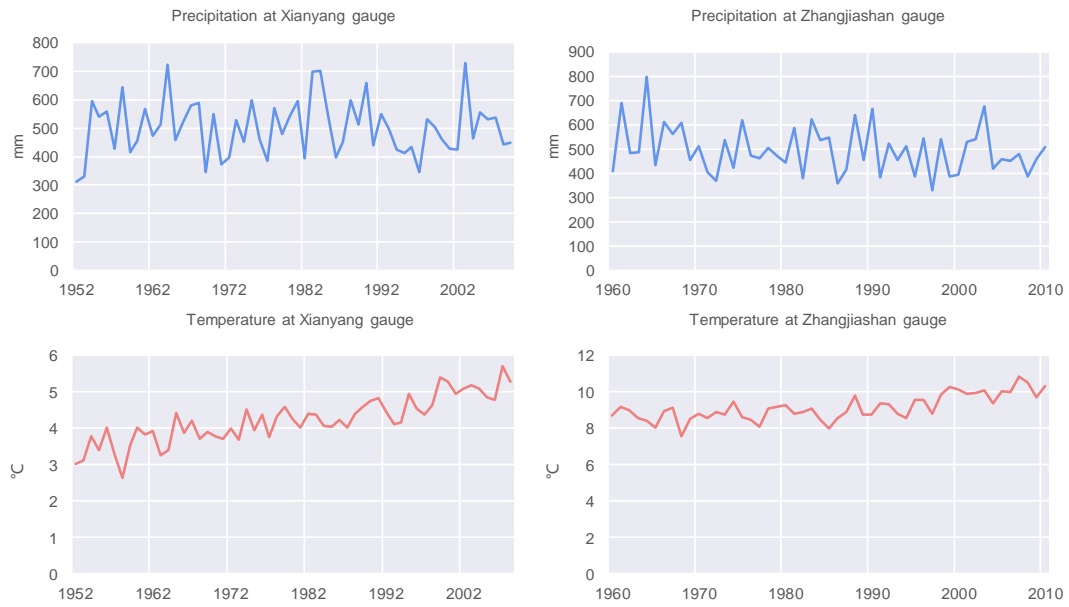


Figure 14. The precipitation and temperature datasets at Xianyang gauge and the Zhangjiashan gauge.

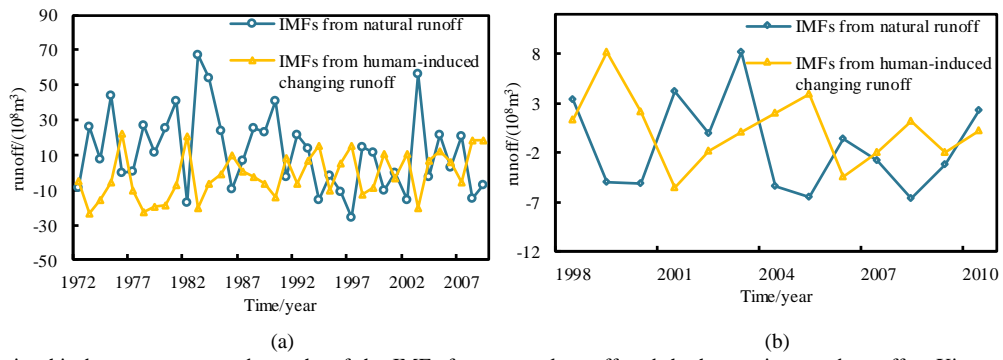


Figure 15. Relationship between crests and troughs of the IMFs from natural runoff and the human-impacted runoff at Xianyang gauge (a) and Zhangjiashan gauge (b).

Table 1. Results of TFPW-MK tests

Gauge	Time (year)	α	P value (two-tailed test)	H_0		
Xianyang	1934-1971 (period-1)	0.001	0.76	0		
		0.005	0.76	0		
		0.01	0.76	0		
		0.05	0.76	0		
		0.1	0.76	0		
		0.5	0.76	0		
	1934-2009 (whole series)	0.001	3.7×10^{-8}	1		
		0.005	3.7×10^{-8}	1		
		0.01	3.7×10^{-8}	1		
		0.05	3.7×10^{-8}	1		
		0.1	3.7×10^{-8}	1		
		0.5	3.7×10^{-8}	1		
		Zhangjiashan	1932-1997 (period-1)	0.001	0.50	0
				0.005	0.50	0
0.01	0.50			0		
0.05	0.50			0		
0.1	0.50			0		
0.5	0.50			0		
1932-2010 (whole series)	0.001	3.1×10^{-4}	1			
	0.005	3.1×10^{-4}	1			
	0.01	3.1×10^{-4}	1			
	0.05	3.1×10^{-4}	1			
	0.1	3.1×10^{-4}	1			
	0.5	3.1×10^{-4}	1			

Note: The result of the test is returned in $H_0 = 1$ (denoting significant trend) indicates a rejection of the null hypothesis (No monotonic trend) at the α significance level. $H_0 = 0$ (denoting no significant trend) indicates a failure to reject the null hypothesis at the α significance level.

Table 2. Optimized predictive factors and their regression parameters in the IMFMGF model

Predictive factors	Regression parameters	Z
$f_2^{(0)}$	-1.392	437873.12
$f_4^{(2)}$	-1.267	434260.76
$f_{19}^{(0)}$	-0.552	385609.55
$f_3^{(1)}$	0.079	203286.13
Precipitation	0.194	
Temperature	0	
a_0	0	

Table 3. Results of TFPW-MK tests for precipitation and temperature at Xianyang gauge and Zhangjiashan gauge.

Gauge	Time series	Z	H_0	
Xianyang	Precipitation	-0.12	0	No significant trend
	Temperature	7.34	1	Upward trend detected
Zhangjiashan	Precipitation	-1.74	0	No significant trend
	Temperature	4.73	1	Upward trend detected

Note: The result of the test is returned in $H_0 = 1$ (denoting significant trend) indicates a rejection of the null hypothesis (No monotonic trend) at the α significance level. $H_0 = 0$ (denoting no significant trend) indicates a failure to reject the null hypothesis at the α significance level.

Table 4. Length of streamflow, precipitation and temperature datasets in the study areas.

Dataset	Xianyang gauge	Zhangjiashan gauge
Streamflow	1934-2009 (76 years)	1932-2010 (79 years)
Streamflow before the abrupt change point (period-1)	1934-1971 (38 years)	1932-1997 (66 years)
Streamflow after the abrupt change point (period-2)	1972-2009 (38 years)	1998-2010 (13 years)
Precipitation	1952-2009 (58 years)	1960-2010 (51 years)
Temperature	1952-2009 (58 years)	1960-2010 (51 years)

*Declaration of Interest Statement

We confirm that this work is original and has not been published elsewhere, nor is it currently under consideration for publication elsewhere. All authors have read and approved the manuscript being submitted, and agree to its submittal to this journal, and have no conflicts of interest to disclose.

The work described in this paper was supported financially by the National Natural Science Foundation of China (51379014), the Major Program of the National Natural Science Foundation of China (41790441) and the Technology Foundation for Selected Overseas Chinese Scholars, Department of Personnel in Shaanxi Province of China (2017035), and the Research Council of Norway (FRINATEK Project 274310).

Detection and attribution of abrupt shift in minor periods in human-impacted streamflow

Tian Lan ^a, Hongbo Zhang ^{b,*}, Chong-yu Xu ^c, Vijay P. Singh ^d, Kairong Lin ^e

^a School of Geography and Planning, Sun Yat-sen University, Guangzhou, 510275, China;

^b School of Environmental Science and Engineering, Chang'an University, Xian 710054, China;

^c Department of Geosciences, University of Oslo, P.O. Box 1047, Blindern, 0316 Oslo, Norway;

^d Department of Biological and Agricultural Engineering & Zachry Department of Civil Engineering, Texas A&M University, College Station 77840, USA;

^e School of Civil Engineering, Sun Yat-sen University, Guangzhou, 510275, China;

*Correspondence: hbzhang@chd.edu.cn

Tian Lan and Hongbo Zhang conceived of the presented idea and developed the theory and performed the computations. Kairong Lin verified the analytical methods. Chong-yu Xu and Vijay P. Singh supervised the findings of this work. All authors discussed the results and contributed to the final manuscript.